Geochemical evidence for arc-related setting of Paleoproterozoic (1790 Ga) volcano-sedimentary and plutonic rocks of the Rombak Tectonic Window

Tine L. Angvik [1, 2], Leon Bagas [3], Are Korneliussen [1]

[1] Norges Geologiske Undersøkelse, Postboks 6315 Sluppen, 7491 Trondheim.
[2] University of Tromsø, Dramsveien 201, 9037 Tromsø
[3] Centre for Exploration Targeting, ARC Centre of Excellence for Core to Crust Fluid Systems, The University of Western Australia, 35 Stirling Highway, Crawley, WA 6009, Australia

ABSTRACT

The Rombak Tectonic Window (RTW) of north-central Norway is an inlier exposed through Caledonian (ca. 500-400 Ma) nappes and represents a western-extension of the Proterozoic Fennoscandian Shield in Sweden and Finland to the east. Sensitive high-resolution ion-microprobe U–Pb dating of zircons from monzogranite samples collected for the study in the RTW yielded ages of ca. 1790 Ma, which are synchronous with granites in Sweden and Finland. Structurally, the granites cross-cut and are cross-cut by large north-going oblique-slip shear zones within the inlier that are associated with Au-sulfide mineralisation. Therefore, the ca. 1790 Ma age brackets both the timing of the deformation and the timing of the gold and sulfide mineralization.

The RTW has a complex geology with a strongly deformed metamorphosed succession of ca. 2000 – 1867 Ma turbidites (greywacke and shale), graphitic shale, quartzite, conglomerate and marble interbedded with metamorphosed ultramafic, mafic, intermediate and felsic volcanic.

Both the sedimentary and volcanic units have similar tectonic settings as indicated by geochemical discrimination affinities, with the sedimentary rocks having being deposited in an active continental margin or island-arc setting, and the ultramafic and mafic plotting in a continental to oceanic-arc settings. The geochemistry of the volcanic rocks also suggests that they were deposited in an island-arc setting over a tonalitic substrate. In addition, they are primitive and probably derived from the mantle. Therefore from the geochemical characteristics of the volcanic rocks, we suggest that the metasedimentary rocks in the RTW were deposited in an island arc to active continental margin setting, from a provenance dominated by mafic to intermediate and felsic volcanic rocks.

The ca. 1790 Ma granitic rocks are late-orogenic to anorogenic and associated with a volcanic-arc to within-plate tectonic setting, which is a similar tectonic setting as the metasedimentary and volcanic units they intrude. It is suggested that these granites are derived by similar rocks as those they intrude and were emplaced during or shortly after the ca. 1850-1800 Ma Svecofennian Orogeny. We also suggest the metamorphosed metasedimentary, volcanic and plutonic rocks in the inlier developed in a long-lived and progressive tectonic event spanning ~70 Ma in an island-arc setting. Through time, the island-arc progressively changed into a continental-arc with felsic volcanic rocks and granites being emplaced. This sedimentary, volcanic and plutonic succession then accreted on to the Baltic continent to the east.

Keywords: Rombak Tectonic Window, tectonic model, Paleoproterozoic, geochemistry, U-Pb zircon dating

1. Introduction

Precambrian rocks in the northern part of Norway are overlain extensively by Caledonian (ca. 500-450 Ma) thrust nappes, and are therefore known principally from geophysical investigations and the study of inliers or “tectonic windows” (e.g. Bergh et al., 2010; Larsen et al., 2013). Archaean and Paleoproterozoic units in these inliers in Norway, Sweden, Finland and northwest Russia are presently assigned to the northern part of the Fennoscandian Shield containing metasedimentary belts intruded by similar aged granites (Fig. 1; Bargel, et al., 1995). The granites are largely coeval and assigned to the Transscandinavian Igneous Belt (TIB; e.g. Romer et al., 1992; Larson & Berglund, 1992; Persson & Wikström, 1993; Wikström, 1996).

The Fennoscandian Shield is an important source for metals and despite centuries of exploration, new deposits are still being explored (e.g. Weihed et al., 2005). A more precise knowledge of the tectonic and metallogenic evolution of the shield is required for the understanding of ore-forming systems in the region leading to a better targeting tool for mineral exploration, and this requires accurate structural and geochronological investigations.

This contribution presents the results of structural, geochronological and integrated geochemical investigations (Korneliussen & Sawyer, 1989; Sawyer & Korneliussen, 1989) in RTW and a model for the crustal evolution of the Fennoscandian Shield in north-central Norway.

2. Regional geology of the Fennoscandian Shield

The RTW is an important Paleoproterozoic terrane in the Fennoscandian Shield containing metallic mineralization (Cu-Fe-Zn-Pb-As-Au) characterised by disseminated massive sulfides along bedding-parallel layers interpreted as possible sedimentary exhalative deposits, in gashes associated with folds and faults, and in steep late-stage anastomosing ductile shear zones (Coller, 2004; Larsen et al., 2010; Whitehead, 2010; Larsen et al., 2013).

The Fennoscandian Shield extends from at least Norway to Russia, and is likely to be a continuation of the Paleoproterozoic successions in the eastern part of Greenland (e.g. Bagas et al., 2013). Inliers of the shield are exposed in windows formed through allochtonous nappes of Paleozoic Caledonian rocks and situated near the southern margin of the Archaean component of the Precambrian Baltic Shield (Gaál and Gorbatschev, 1987; Gorbatschev, 1985; Gustavson and Gjelle, 1991; Romer et al., 1991; Myers and Kroner, 1994). The nappes are the products of collisional tectonics during the Early to Mid-Paleozoic that was followed by extensional collapse during ca. 400-350 Ma (e.g. Fossen, 2000). Four Caledonian nappes were thrust over the Baltoscandian Platform in Norway mainly to the southeast (e.g. Gee & Sturt, 1985). These structures are characterized by their flat lying nature as compared to the steeply dipping foliation within the inliers (e.g. Birkeland, 1976). Erosional processes gradually exposed the underlying tectonic inliers such as the RTW (Fig. 1).

RTW consists of a succession of metamorphosed volcanic and sedimentary rocks that formed parts of the Paleoproterozoic (ca. 2000 – 1867 Ma) Bothnian Basin located between central Sweden to the eastern part of Finland (Lindquist, 1987; Welin

et al., 1993; Korneliussen and Sawyer, 1989). Mafic dykes, granodiorite, monzogranite and syenite, which are the predominant rock types in the inlier, intrude these basement rocks (Gaál and Gorbatschev, 1987; Nironen, 1997; Fig. 2).

RTW is an important transition between the autochthonous northeast and eastern part of the Fennoscandian Orogen and the exposed basement rocks located west of the Caledonides, such as the West Troms Basement Complex (WTBC) and Mauken Tectonic Window (Fig. 1). As yet, the relationship between the disparate windows in the orogen and the nature of the Paleoproterozoic crustal architecture related to the Svecofennian crustal scale shear zones are poorly understood.

Six narrow zones of north-trending amphibolite facies metasedimentary and metavolcanic rocks, including metamorphosed greywacke, quartzite, graphitic shale and carbonate, form linear rafts in granite in the RTW. The age of the rafts is not known, but they are younger than the ca. 1951 Ma tonalites and older than ca. 1800 Ma granites (Skyseth and Reitan, 1990; Romer et al., 1991). In addition, regional metamorphism took place in the tectonic windows during the ca. 1850-1800 Ma Svecofennian Orogeny (e.g. Korsman et al. 1984; Nironen, 1997), which was followed by greenschist-facies retrogression associated with folding and ductile faulting between (Sawyer, 1986; Korneliussen et al., 1989).

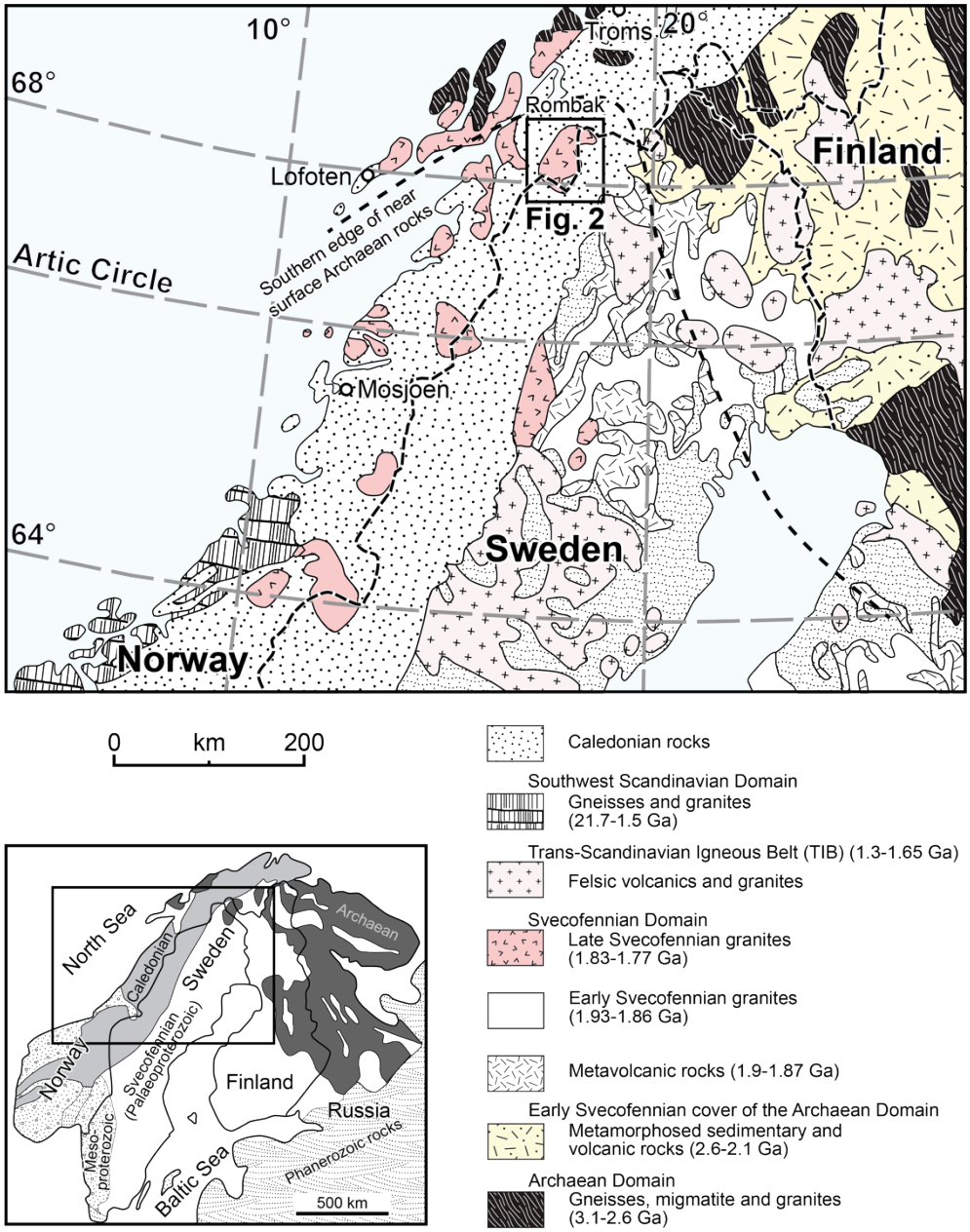

Fig. 1. Geology of the central part of Norway showing the location of the Rombak Tectonic Window shown in Fig. 2 (modified after Gaál and Gorbatschev, 1987).

3. Tectonic geology

3.1. Regional tectonics

Rocks in the Fennoscandian Shield have been deformed during the Svecofennian Orogeny associated with the collision or accretion of at least two continents (Nironen, 1997; Korja et al., 2006; Lahtinen et al., 2008).

Hietanen (1975) was the first person to suggest that the Svecofennian Orogen had an island-arc tectonic setting before the onset of collision. The orogen is still interpreted as a collage of microcontinents and island arcs accreted on to the Karelian microcontinent which itself was accreted onto the North Atlantic Craton (NAC) during ca. 1.8 Ga (Nironen, 1997; Korja et al., 2006). The geometry of these microcontinents is still unknown as the mappable continuity of the juxtaposing shear zones and lithologically units are masked by the overlying Caledonian sequences. Korja et al. (2006) proposed that the accretion of the microcontinents and island-arcs evolved in the following stages: 1) microcontinent accretion between ca. 1920 and 1880 Ma; 2) large-scale extension of the accreted crust between ca. 1870 and 1840 Ma; 3) continent-continent collision during ca. 1870-1790 Ma); and 4) gravitational collapse between ca. 1790 and 1770 Ma.

Nironen (1997) describes how convergent deformation associated with the collision of continent and island-arc complexes during the Svecofennian Orogeny resulted in partitioning of transpressional and ductile shear zones with the development of several crustal scale ductile shear zones within the Bothian Basin. The deformation events assigned to the orogeny have affected the basement and intrusive rocks in varying degrees across the RTW and other inliers in Norway and

Sweden (Fig. 1). On a shield scale, fabrics assigned to the deformation include early regional, north-trending and steeply dipping, dextral oblique and strike-slip shear zones (e.g. Lindh, 1987; Berthelsen and Marker, 1986; Nironen, 1997; Braathen and Davidsen, 2000; Olesen and Sandstad, 1993; Henderson and Kendrick, 2003). These shear zones have been locally sinistrally reactivated (Berthelsen and Marker, 1986; Kärki and Laajoki, 1995).

Bergh et al. (2010) provide the most comprehensive study of a complex set of anastomosing Paleoproterozoic shear zones in the WTBC, which are interpreted as part of a complex and multiphase Paleoproterozoic amalgamation of both Archaean and Paleoproterozoic microcontinents to the west of the Caledonides. They describe an initial orthogonal to oblique phase of NW-SE directed compression producing a NW-verging fold and thrust belt, which was subsequently transposed by a predominantly sinistral oblique set of steep ductile shear zones in a progressive transpressional orogen. Various authors interpret similar evolutionary tectonic events in the region (Braathen and Davidsen, 2000; Myhre et al., 2011, Henderson and Viola, 2013).

3.2 Local deformation in the Rombak Tectonic Window

Ductile shear zones in the RTW vary on a millimetre- to kilometre-scale and extend ≥60 km in length disappearing beneath Caledonian thrusts to the north and south (Fig. 2; Larsen et al., 2010, 2013). These structures have complex geometries and are observed as narrow, high-strain zones made up of anastomosing steep, northerly trending, oblique-slip ductile shear zones that segment and juxtapose zones of low-strain. The zones contain remnants of tight, upright, east-verging fold and thrust faults, which thicken and repeat the metasedimentary sequences. The high-

strain oblique-slip shear zones are localized along the margins of the metamorphosed volcanic and sedimentary rocks and plutonic intrusions (Larsen et al., 2010; 2013).

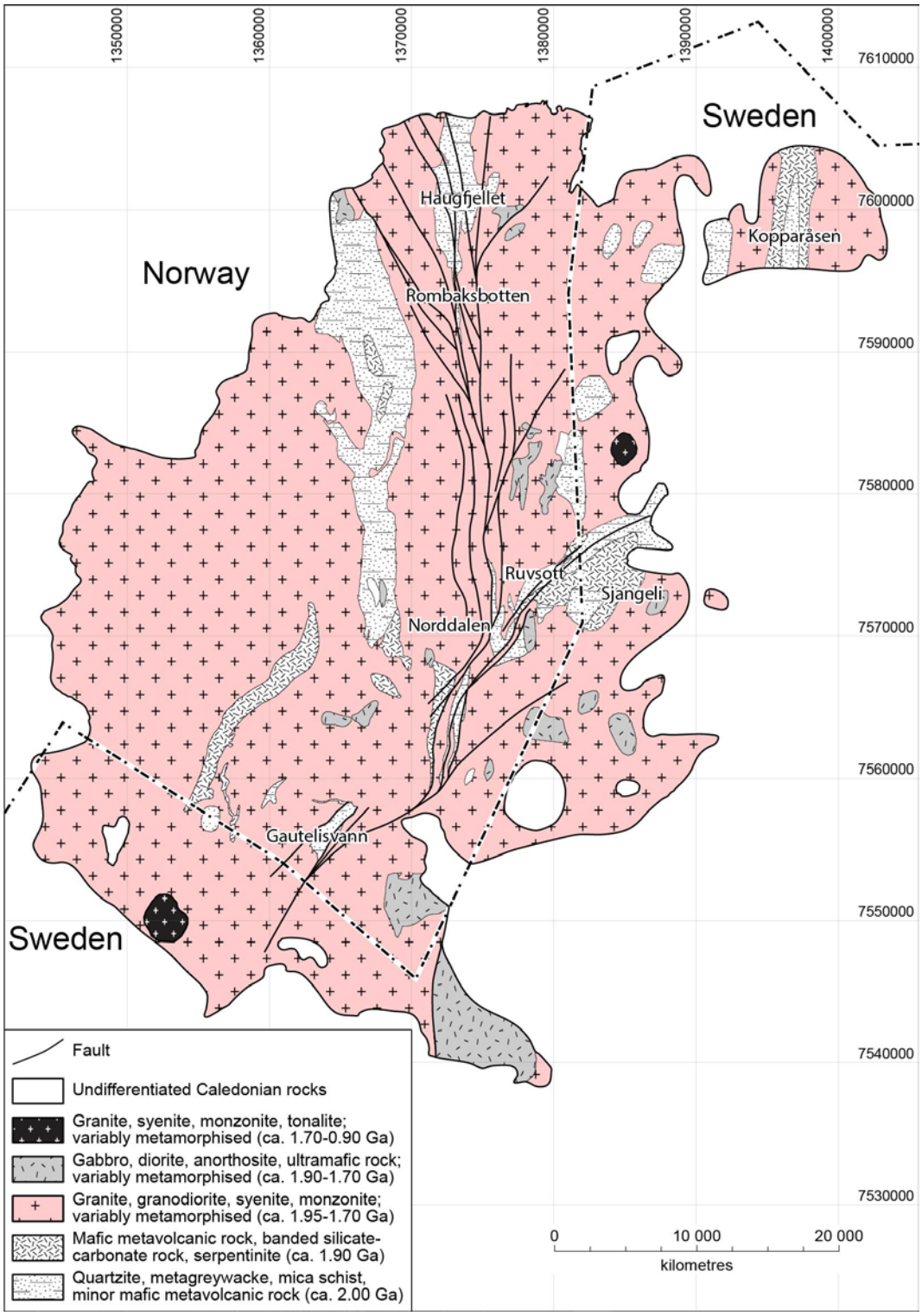

Fig. 2. Geology of the Rombak Tectonic Window (from Larsen et al., 2013 modified after Bargel et al., 1995).

The steeply dipping high-strain shear zones post-date and segment the earlier phase of dip-slip movement. These high-strain shear zones display a complex range of kinematics, including reverse dip-slip, dextral and sinistral oblique-slip, and ductile kinematic indicators including sigma clasts, crenulations cleavages, brittle-ductile tension gash fractures and asymmetric boudinaged that are suggestive of multiple periods of movement with an overall dextral transpressional sense of movement. From detailed kinematic studies, these structures are interpreted to represent a protracted, east-directed oblique transpression during Paleoproterozoic accretionary tectonics (Larsen et al., 2010).

A complex structural history of the accretionary system is interpreted to the following progressive stages: (1) formation of an orthogonal, east-verging fold and thrust belt with simple horizontal open, asymmetric F_1folds, and accompanying gently west-dipping thrusts; (2) coaxial refolding and formation of gently N-S plunging F_2 folds; (3) F_2 folds are cut by steeply dipping, N-trending, sinistral anastomosing and axial planar ductile oblique-slip shear zones; and (4) development of steeply dipping, dextral northeast-trending ductile oblique-slip shear zones. These late shear zones are associated with steep plunging F_4 folds and cut and complexly segmenting both the earlier formed upright fold and thrust belt structures and the sinistral ductile shear zones (Larsen et al., 2010; 2013).

Various granitic bodies intrude and are located close to the shear zones within this complex structural evolution. The shear zones cut the fold-and-thrust structures and some of the oblique-slip shear zones. Based on the structural and intrusive relationships, the structures have been interpreted to be coeval with syn- to late-orogenic intrusions (Larsen et al., 2013).

Here we present geochemical data from the rocks and U-Pb age dating study of these granitic bodies documenting a progressing tectonic evolution in the RTW during the Paleoproterozoic. The granitic bodies crosscut the late and steep oblique shear zones (D_4), which gives a minimum age for the Rombaken Skjomen Shear Zone (RSSZ) and a frame for understanding metallogenic processes in the region.

4. Methodology

4.1. Whole-rock geochemistry

The Norges Geologiske Undersøkelise (NGU, Norwegian Geological Survey) collected 46 samples of metasedimentary, metavolcanic and intrusive rocks from Haugfjellet, Rombak, Norddalen Ruvvsott, Sørdalen and Gautelisvann (Fig. 2; also see Korneliussen et al., 1986; Korneliussen and Sawyer, 1989; Sawyer and Korneliussen, 1989). The samples have been analysed by the NGU, Institute for Energy Technology and Midland Earth Science Associates.

Major oxides concentrations were determined using a wavelength-dispersive XRF on fused disks (after Norrish and Hutton, 1969). Trace elements Y, Zr, Nb, Rb, Ba, Sr Pb, V, Cu, Zn, and Ni were determined by wavelength-dispersive XRF on a pressed pellet (after Norrish and Chappell, 1997). Sc, Co, Cr, Cs, Hf, Ta, Th, U, La, Ce, Nd, Sm, Eu, Tb, Yb and Lu, were analysed by instrumental neutron activation analysis (NAA).

The geochemical data for these rocks are presented in the Appendix. Despite variable degrees of recrystallization, the mafic igneous rocks have consistent concentrations of immobile elements such as La, Nb, Y, and Zr. However, relatively

mobile elements show wide variations in their analyses attributed to alteration and metamorphism, and interpretations based on elements such as Sr, Ba, Na, K, and Ca have thus been avoided.

4.2. SHRIMP U-Pb zircon dating

Zircon crystals are handpicked from the heavy mineral separate with the aid of a binocular microscope. In general, up to 200 representative crystals are selected from igneous and sedimentary rocks. Crystals are mounted in 25 mm diameter Epofix epoxy disks, and the mount surface polished to expose grain interiors.

Each mount contains zircons from three different samples, which are aligned in rows, together with BR266 and OGC1 used as U–Pb calibration standard zircons.

Mount-making and backscattered electron and cathodoluminescence (CL) imaging were completed at the Centre for Microscopy, Characterization and Analysis at the University of Western Australia. Gold coating of mounts were performed at the John de Laeter Centre, Curtin University in Western Australia.

Zircon grains were analysed using the SHRIMP-II facility housed within the John de Laeter Centre for Mass Spectrometry at Curtin University of Technology. Procedures for SHRIMP U–Pb isotopic analysis followed those described by Compston et al. (1984),and Stern (2009). Targeted grains were sputtered using an O_2^- primary beam with a 30 μm–diameter spot, and six cycles of sequential measurements of peaks in the secondary ion beam at mass stations 196 ($^{90}Zr_2O^+$), 204 ($^{204}Pb^+$), 204.1 (background), 206 ($^{206}Pb^+$), 207 ($^{207}Pb^+$), 208 ($^{208}Pb^+$), 238 ($^{238}U^+$), 248 ($^{232}ThO^+$) and 254 ($^{238}UO^+$) were made using an electron multiplier in pulse counting mode.

The effect of Pb/U fractionation in measurements of the unknowns was corrected by reference to interspersed analyses of the laboratory U–Pb standard zircon BR266 (U = 909 ppm, $^{207}Pb/^{206}Pb$ age = 559; Stern, 2001) and OGC1 ($^{207}Pb/^{206}Pb$ age = 3465 Ma; Stern et al., 2009).

The measured ^{204}Pb was used for common Pb correction. The data was compiled using the ISOPLOT 3.0 and Squid 1.0 programs (Ludwig, 2003, 2009). Individual analyses are reported with 2σ uncertainties; weighted averages of age are also reported at the confidence of 2σ.

5. Results

5.1 Geochronology

Three samples (NO13, GL19 and HF1) of granite were collected from the RTW for SHRIMP U-Pb zircon dating (Fig. 3). The aim of this exercise was to determine whether they represent a Paleoproterozoic or Caledonian (ca. 490-390 Ma) magmatism, and to help petrographically outline the tectonic events in the region.

Sample NO13 is a sample of monzogranite collected from Norddalen. Zircons analyzed are euhedral, elongated or stubby, most show oscillating zoning typical of magmatic zircons, and most have a homogeneous pool of ages with a weighted mean of 1786 ± 8 Ma (MSWD = 0.38, n = 16; Fig.3a).

Sample GL19 is from monzogranite collected from Gautelisvann. The zircons are similar in shape and zonation to sample NO13 and the main population yields an upper intercept age of 1789 ± 4 Ma (MSWD = 1.2, n =24), and there is a scatter of younger ages due to Pb loss (Fig. 3b).

Sample HF1 is of a monzogranite from Haugfjellet. The zircons are stubby to elongate (Fig. 4), and zircon analyses yield a weighted mean of 1790 ± 8 Ma (MSWD = 0.27, probability 0.99, n = 18; Fig. 3c). These three dates are the same within error and indicate a significant magmatic event of ca. 1790 Ma.

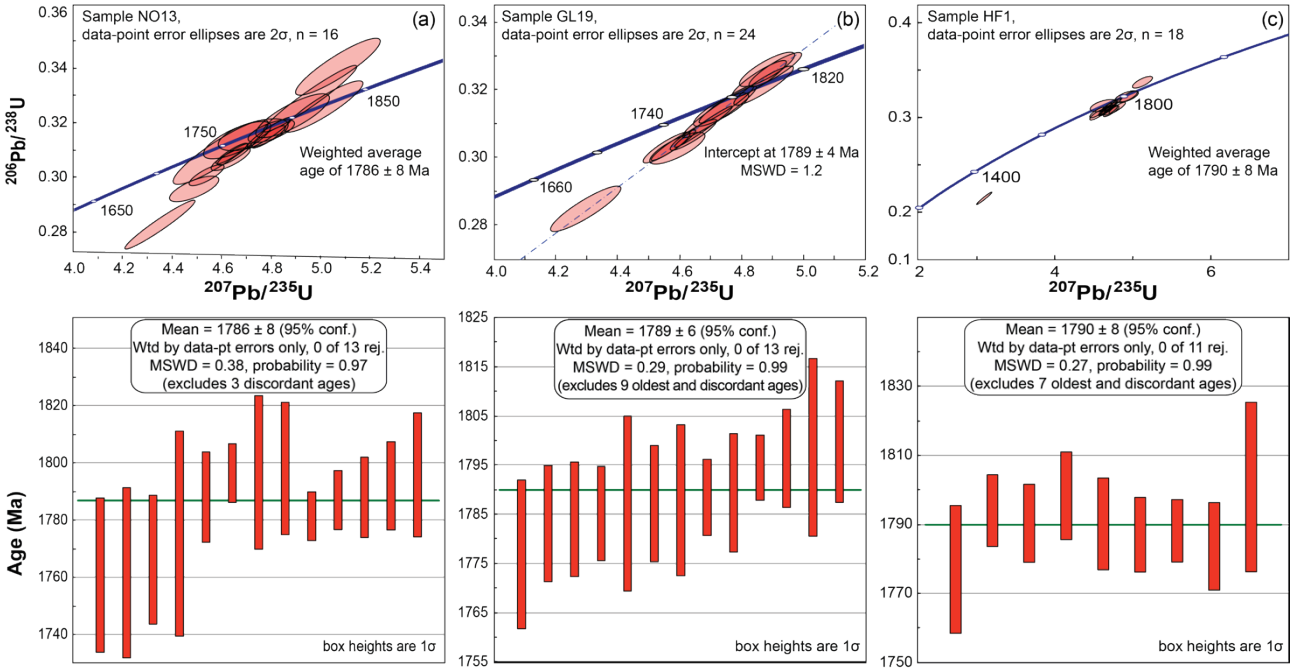

Fig. 3. U-Pb concordia diagrams for SHRIMP results and Weighted means for: (a) Sample NO13; (b) Sample GL19; and (c) Sample HF1; n is the number of zircon ages in the calculated age. Error ellipses represent 2 σ uncertainties.

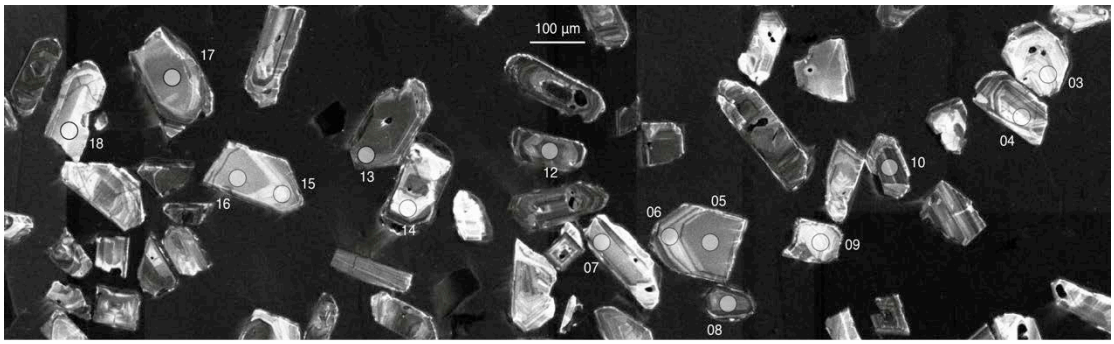

Fig. 4. Scanning electron microscopy cathodoluminescence (CL) image of zircons from Sample HF1 showing the location of spots with SHRIMP U-Pb analyses.

5.2. Geochemistry of greywacke and shale units

Sawyer and Korneliussen (1989) and the researchers of this study collected 18 samples of greenschist to amphibolite facies, siltstone, and fine- to medium-grained lithic sandstone. The samples came from surface exposures in the Rombaksbotten (6), Gautelisvann (4), Ruvssot (4) areas and were collected for geochemistry (Appendix A-1). Despite variable degrees of recrystallization, the rocks show relatively limited compositional variation.

It is assumed that rare earth element (REE) abundances and patterns in clastic sedimentary rocks trace the chemical evolution or development of the upper continental crust since Precambrian times. It is also that the average composition of the upper crust is not significantly different from the average composition of the Precambrian crust (e.g. Moorbath, 1977; Armstrong and Harmon, 1981; Taylor et al., 1981). These two hypotheses assume: (a) the REE have not experienced relative fractionation during weathering, erosion, deposition and diagenesis accompanying the transformation of source rocks into sediment; (b) metamorphism has not altered the whole-rock REE patterns of the samples; (c) the REEs in sedimentary rocks provide a broad average of available source areas at the time of sedimentation; and (d) the sampled units are representative of sediments deposited in the area.

Applying a geochemical classification plot (K_2O/Na_2O versus SiO_2/Al_2O_3) of Wimmenauer (1984), the Paleoproterozoic samples can be classified as greywackes, arkoses, and pelitic greywackes (Fig. 5).

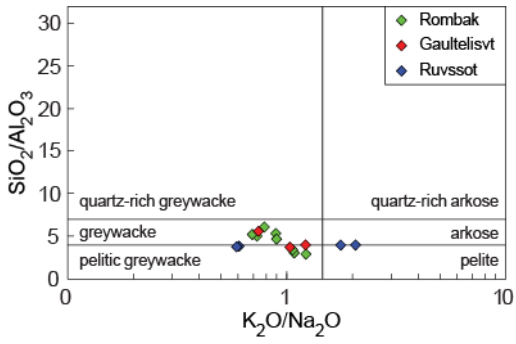

Fig. 5. Metagreywacke and pelite samples from Rombaksbotten, Gautelisvann and Ruvssot in the geochemical classification plot after Wimmenauer (1984).

The samples show a spectrum of chemical compositions resembling that of the upper crust (Fig. 6a; Rudnick and Gao, 2004), and have geochemical compositions that are free of anomalously high concentrations of Ti, Zr, Hf and Y (Fig. 6b and c). These elements would be concentrated by hydraulic sorting of heavy minerals during processes of transportation and deposition of detrital material obscuring relations to the sources of such material (e.g. Cullers et al., 1987).

The normalised geochemical pattern for the Paleoproterozoic sedimentary rocks in the study area broadly resemble the North American Shale Composite (NASC; Gromet et al., 1984), except for the elevated Cr values, Mn depletion, and elevate Na values (Fig. 6b and c). These characteristics suggest that there is a mafic or ultramafic input in the provenance for the rocks, alteration has lead to depletion in Mn, and the rocks might have been affected by saline solutions either as hydrothermal fluids or during deposition.

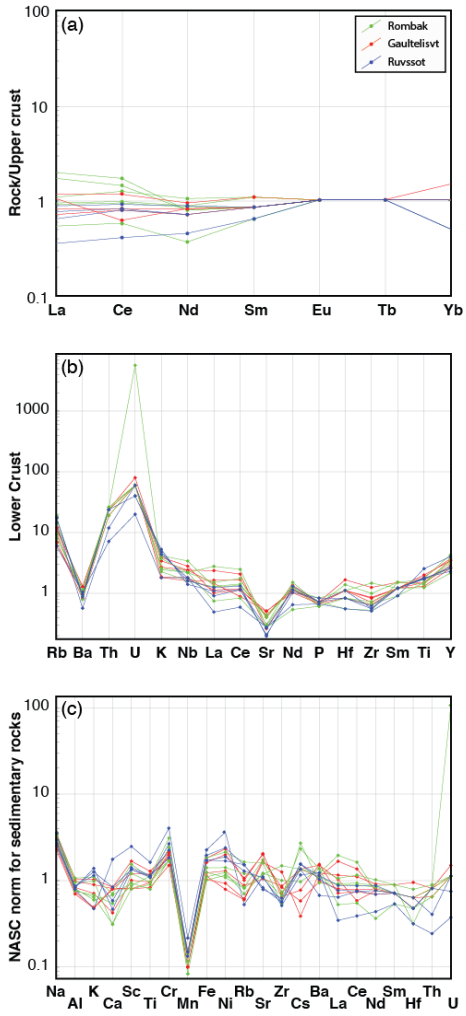

Fig. 6. Geochemical plots for sedimentary rocks in the Rombaksbotten, Gautelisvann and Ruvssot areas: (a) Upper crust normalized (Rudnick and Gao, 2004); (b) Lower Crust normalized (Weaver and Tarney, 1984) showing depletion in Sr and elevation in Th and Rb; and (c) North American Shale Composite normalized (after Gromet et al., 1984) showing depletion in Mn and enrichment in Na.

5.3. Geochemistry of mafic and ultramafic rocks

Basaltic magmatism is a feature of many geotectonic environments in modern intra-oceanic and intracontinental settings as well as at convergent and divergent plate margins (e.g. Wilson, 1989). Geochemical data for 12 mafic intrusive rocks from Gautelisvann and Norddalen, and five komatiites from Ruvssot collected by Korneliussen and Sawyer (1989) have been plotted on discrimination diagrams in an

attempt to help determine what the tectonic environment was during their emplacement.

The spread in the K_2O verses MgO and Na_2O verses MgO plots in Fig. 7 indicates that hypogene alteration (presumably due to either amphibolite facies metamorphism or associated with hydrothermal events) has affected the more mobile elements that might be used as tectonic discriminators. In addition, samples with LOI values above 2% have been disgarded. In order to ascertain the geotectonic setting for mafic units the geochemical data presented in Appendix A-2 are compared against modern analogues of basaltic volcanic rocks using relatively immobile elements. The assumption is that hydrothermal alteration processes in the area did not involve very high fluid/rock ratios that lead to the mobility of where relatively immobile elements (e.g. Lesher et al., 1986; Schandl et al., 1995).

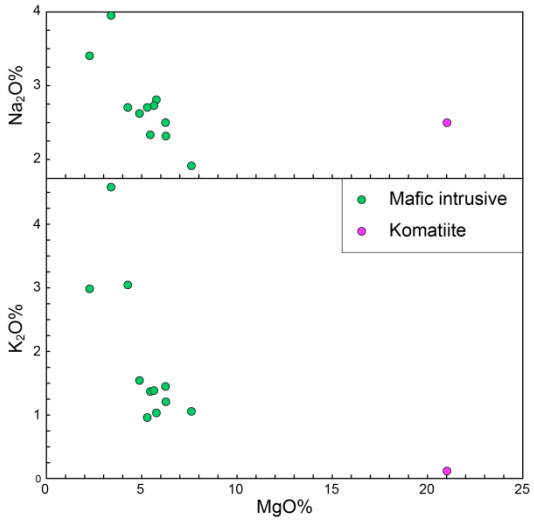

Fig. 7. Plots for mafic and ultramafic rocks from Gautelisvann and Ruvssot: (a) MgO verses Na_2O; and (b) MgO verses K_2O. The spread in the plots suggests that alteration has affected the more mobile elements.

From the Zr/TiO_2–Nb/V classification plot of Winchester and Floyd (1977) shown in Fig. 8, the mafic igneous rocks analysed from the study area predominantly have

basaltic compositions.

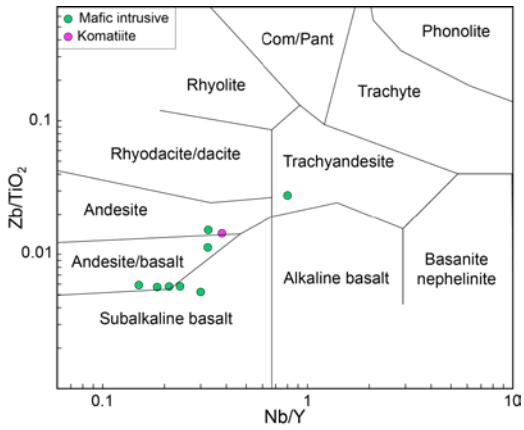

Fig. 8. The Zr/TiO**2**–Nb/V classification plot (after Winchester and Floyd, 1977) for mafic and ultramafic rocks analysed from the study area. These plots rely on relatively immobile elements under a range of alteration and metamorphic conditions. Such plots are commonly used for the classification of ancient or altered volcanic rocks.

On the AFM (Miyashiro 1974, Fig. 9a), FeO*/MgO versus SiO_2 (after Miyashiro, 1974; Fig. 9b), FeO*/MgO versus FeO* (after Miyashiro, 1974; Fig. 9d), and Zr versus Y (after Barrett and MacLean, 1999;l Fig. 9e) diagrams, the samples plot in the tholeiitic field (except for the komatiite samples).

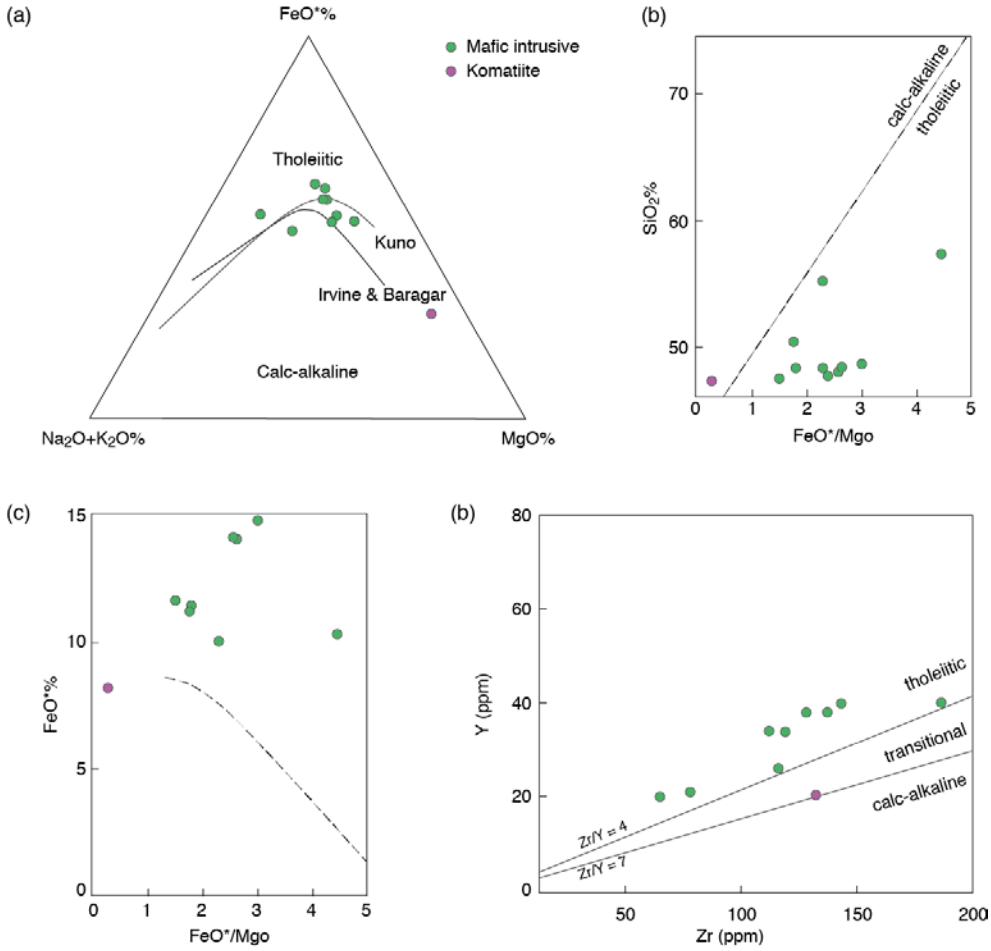

Fig. 9. Plots for mafic and ultramafic volcanics: (a) AFM diagram (after Miyashiro, 1974), (b) FeO*/MgO vs SiO_2% diagram (after Miyashiro, 1974), (c) FeO*/MgO vs FeO* diagram (after Miyashiro, 1974), and (d) Zr vs Y diagram showing that the bulk of the samples have a tholeiitic geochemical affinity. The total Fe is presented as wt % FeO (FeO*).

5.4. Geochemistry of the ca. 1790 Ma felsic igneous rocks in the Rombak Tectonic Window

In general, the ca. 1790 Ma granitic rocks in the Gautelisvann and Norddalen areas in the RTW range in composition from syenite to granodiorite and monzogranite, although monzogranite predominates (Fig. 10a, b). The aluminium saturation index of Barton and Young (2002) indicates that most of the granites have

metaluminous to weakly peraluminous compositions (Fig. 10c). The samples have K_2O contents of 1.5-5.8% (with an average of 4.4%), with the data plotting in alkaline and subalkaline fields in Fig. 10a, in the medium-K calcalkaline and shoshonite series in the K_2O versus SiO_2 classification diagram of Peccerillo and Taylor (1976) in Fig. 10d, and form calc-alkaline trends in the AFM diagram of Fig. 10e (Rollinson, 1996). The rocks also have Al_2O_3 contents between 12.4 and 18.5% (with an average of 14.6%), and TiO_2 contents of 0.09-5.4% (with an average of 0.8%; Appendix A-3).

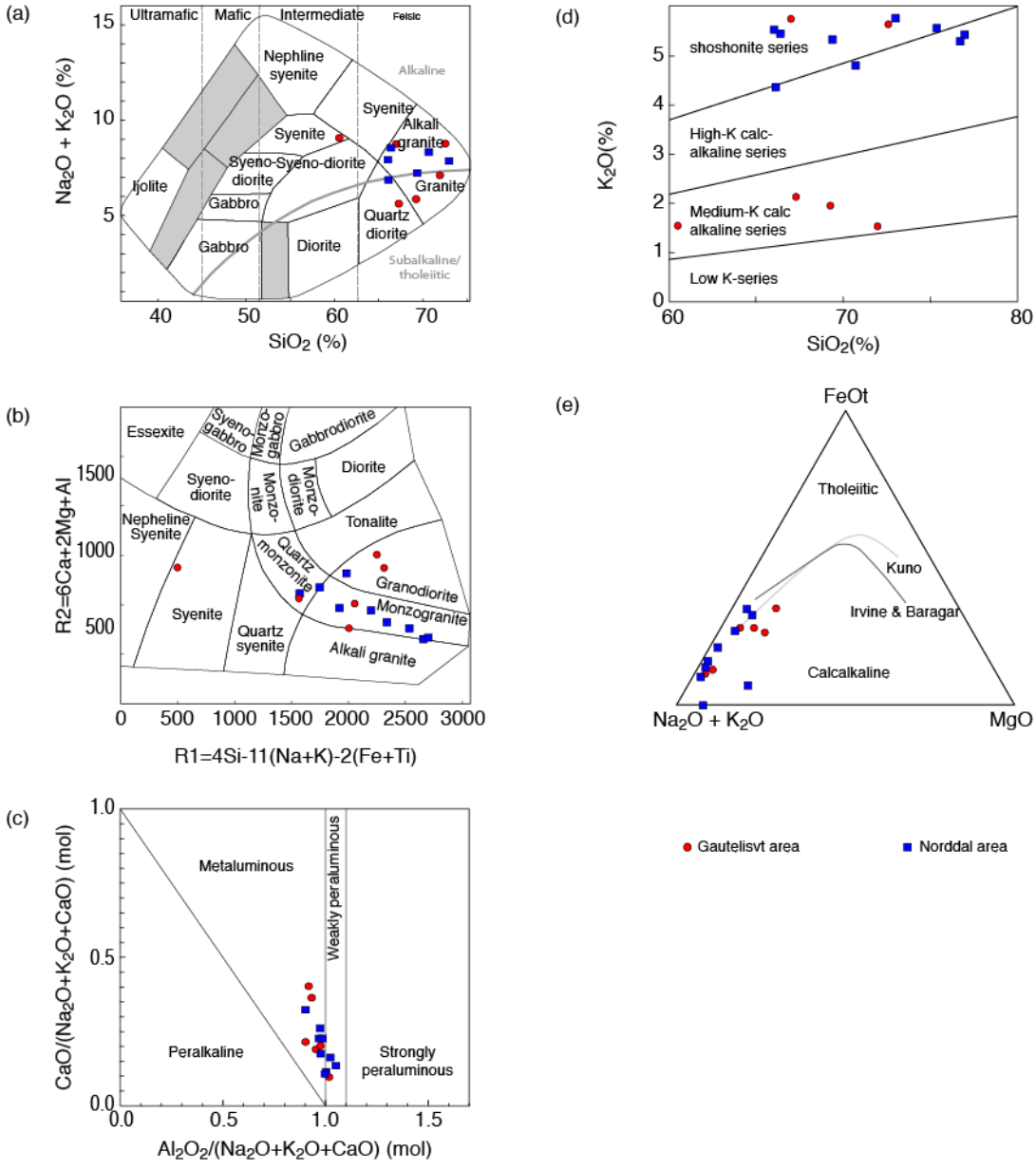

Fig. 10. Classification diagrams for the ca. 1790 Ma granitic rocks from the Gautelisvann and Norddalen areas of the Rombak Tectonic Window: (a) and (b) total alkali versus silica plutonic plot of Cox et al. (1979) and R1 versus R2 plutonic chemical plot of de la Roche et al. (1980) showing that the granites are predominantly monzogranites and granodiorites, with one syenite sample; (c) aluminia saturation of Barton and Young (2002) showing that the samples are metaluminous to weakly peraluminous; (d) K_2O versus SiO_2 classification diagram of Peccerillo and Taylor (1976) showing that the samples can be subdivided into medium-K alkaline series (predominantly from Gautelisvann) and shoshonite series; and (e) AFM diagram of Rollinson (1993) using curves after Irvine and Baragar (1971) and Kuno (1968) showing that the samples form calc-alkaline trend.

The samples also form a linear trend in the ternary diagram Al_2O_3 – CaO+Na_2O – K_2O of Nesbitt and Young (1989) in Fig. 11a. This linear trend indicates that: (i) there is a gradual change in the ratio of CaO + Na_2O to K_2O from the Gautelisvann area to the south to the Norddalen area to the north in the RTW; and (ii) weathering has had minimal overall effect on the samples collected. The plots in Fig. 11b define broad linear trends interpreted to reflect magmatic processes. The broad deviations from linearity in the various Harker (1909) diagrams are considered to reflect variations in initial bulk compositions and compositions of crystallizing phases (Fig. 11b).

The Harker plots in Fig. 11b indicate that: (i) the SiO_2 content varies between 60 and 77%, and the samples plot in the medium- to high-K and shoshonitic fields (also see Fig. 10d); (ii) the granites are heterogeneous; and (iii) the overall patterns of decreasing Ti, Fe, Mg, and Ca with increasing SiO_2 is typical of fractionating granitic systems (e.g. Drake and Weill, 1975; White and Chappell, 1983).

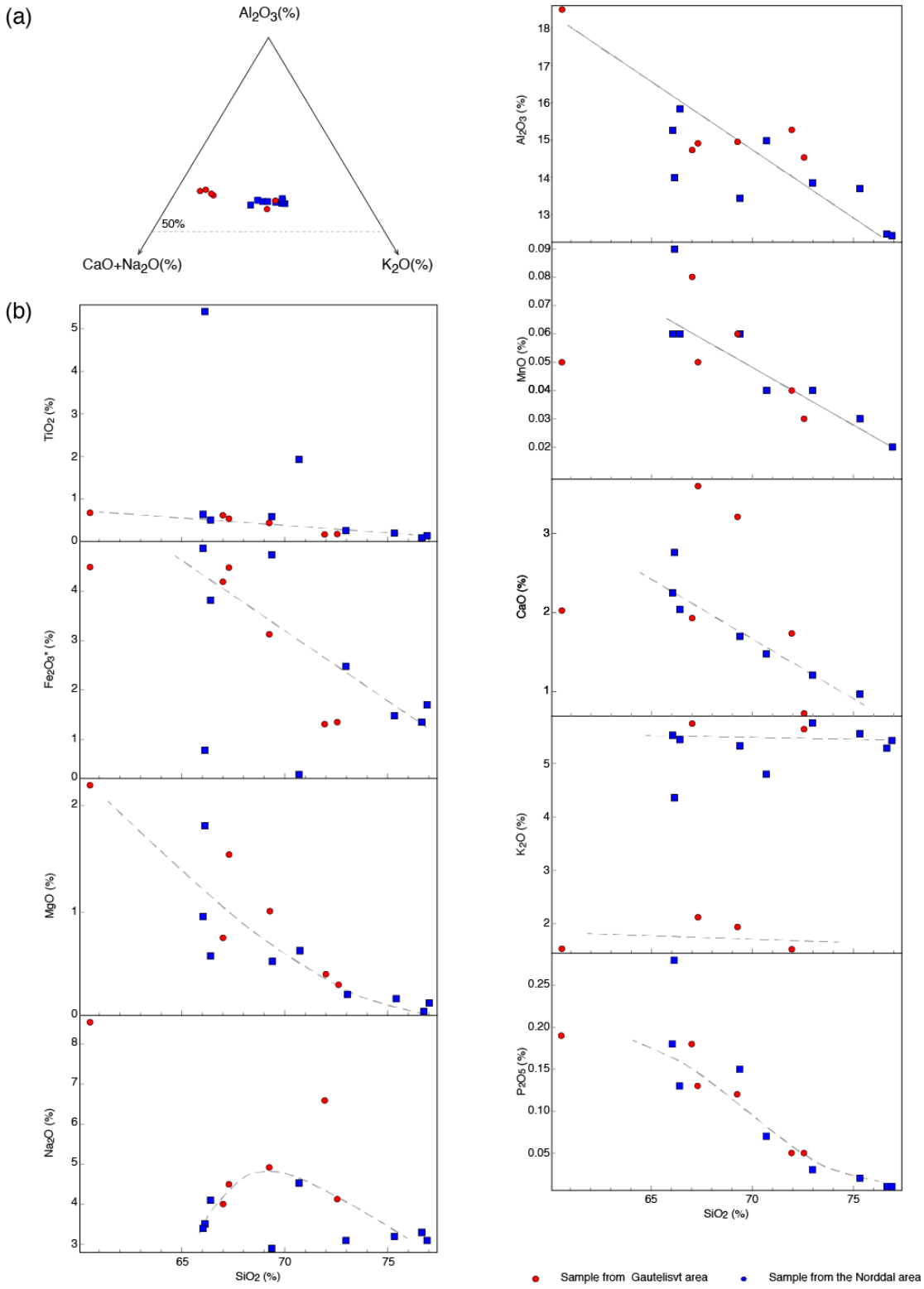

Fig. 11. Diagrams for granites from the Rombak Tectonic Window of Norway: (a) Al_2O_3 – $CaO+Na_2O$ – K_2O (modified from Nesbitt and Young, 1989); (b) Harker (1909) variation diagrams of the major element oxides. The legend is the same for all the diagrams.

Using the ACF diagram of Chappell and White (1974) and White and Chappell (1983), the major element compositions and petrographic observations of the granites noted are not consistent with S-type granites (i.e. of sedimentary origin; Fig. 12a). However, this “S-type” classification is genetic (e.g. Frost et al., 2001), and implies no magma mixing and no fractionation (Bonin, 2007). Furthermore, Fig. 12a assumes that the granites are neither fractionated I-types nor anorogenic (A-type), but most of the samples plot in the I-type granite field of Fig. 12b and the I-type and A-type fields of Fig. 12c indicating that these granites are I-type granites and most are A-types.

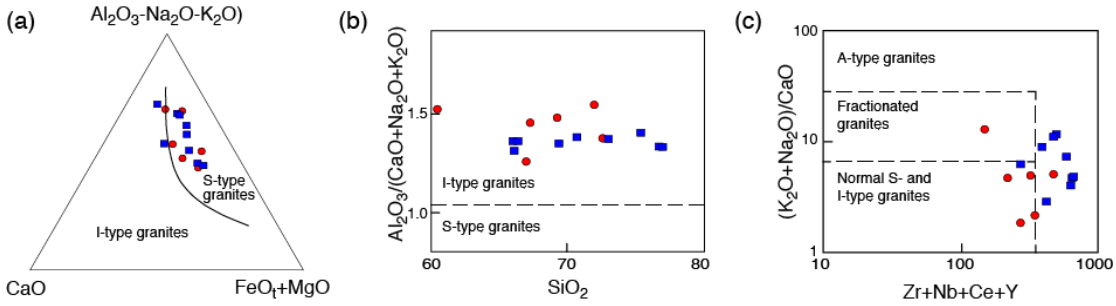

Fig. 12. Compositional diagrams for granites from Rombak Tectonic Window: (a) Al_2O_3-Na_2O-K_2O – CaO – FeO_t+MgO plot of White and Chappell (1983); (b) A1$_2$O3 / (CaO+Na_2O+ K_2O) versus SiO_2 plot of White and Chappell (1983); and (c) (K_2O + Na_2O)/CaO versus Zr + Nb + Ce + Y diagram after Whalen et al. (1987) for fractionated granites (the legend is the same as in Fig. 10).

The granitic rocks have downward-sloping primitive mantle-normalized ‘spidergram’ profiles with large ion lithophile (LILE) enrichment, relative negative Ba, Nb, Sr and Ti anomalies, and positive Th, U and Pb anomalies (Fig. 13a). On MORB normalized plots, Rb, Th, and Ce are anomalous (Fig. 13b). Sr is present in K-feldspar and plagioclase, and is relatively depleted in fractionating melts by the removal of K-feldspar and plagioclase from the system. Rb, however, is commonly present in K-feldspar, biotite and muscovite (McCarthy and Hasty, 1976). Ba is hosted by biotite and K-feldspar, and early fractionation of K-feldspar will deplete the

residual melt in Ba once saturation is reached (McCarthy and Hasty, 1976). Thus, crystal fractionation involving feldspar leads to depletion of Ba and Sr, and enrichment in Rb. The observed patterns suggest that at least some of the granites in the RTW show evidence of fractionation of feldspar and, to a lesser extent, biotite (as is shown by the decreasing Ba and Sr in Fig. 13).

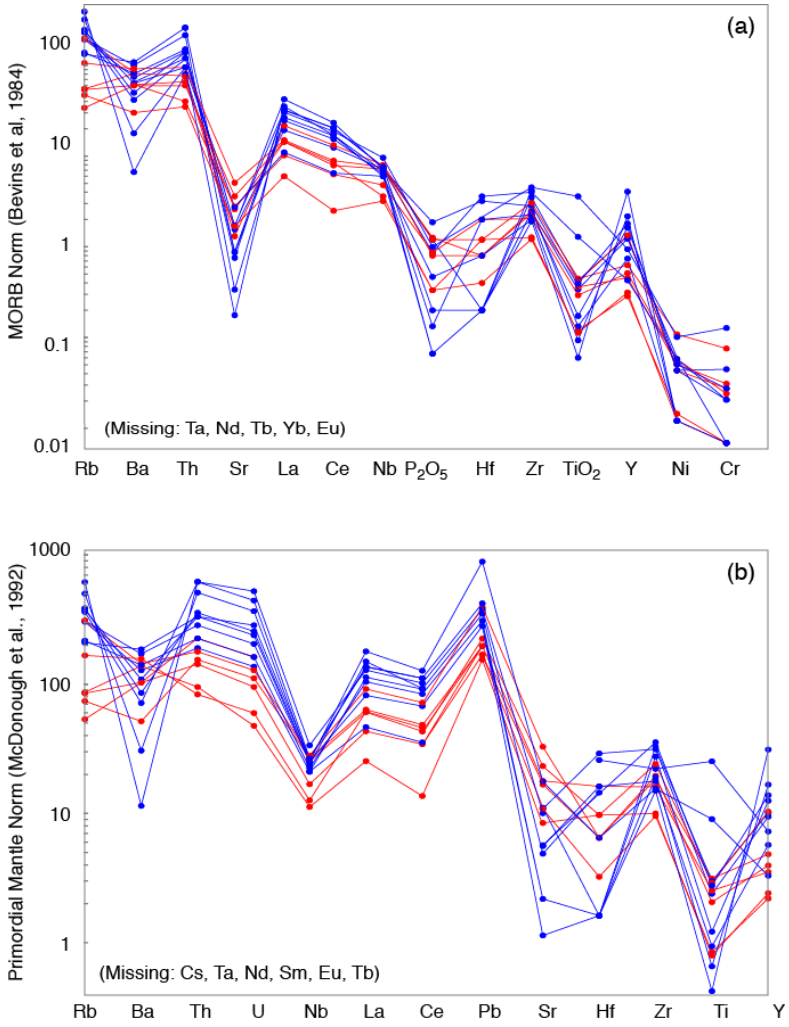

Fig. 13. REE and spider diagrams for granites from the Rombak Tectonic Window: (a) MORB normalized values from Bevins et al. (1984), and (b) Spider diagram for primitive mantle normalized values from McDonough et al. (1992). The legend is the same as in Fig. 10.

6. Paleoproterozoic tectonic setting

6.1. Tectonic setting for the turbiditic sandstone (greywacke) and shale units

Systematic variations in the geochemical compositions of greywackes have been in different tectonic environments to help determine their tectonic setting during deposition (e.g. Bhatia, 1983, 1985a, 1985b; Bhatia and Cook, 1986; Cullers et al., 1987; McLennan et al., 1993). Using such analyses with the least mobile elements, the samples from the Rombaksbotten, Gautelisvann and Ruvssot inliers plot in the continental- to oceanic-arc tectonic setting (Fig. 14a). A similar result is obtained in the general immobile elements Zr, Sc, Th, and La plots in Fig. 14b. These plots also suggest that the samples have possibly been enriched in iron causing them to spread further to the right in right in Fig. 14a, which is consistent with the presence of pyrite in the samples (as observed in thin section).

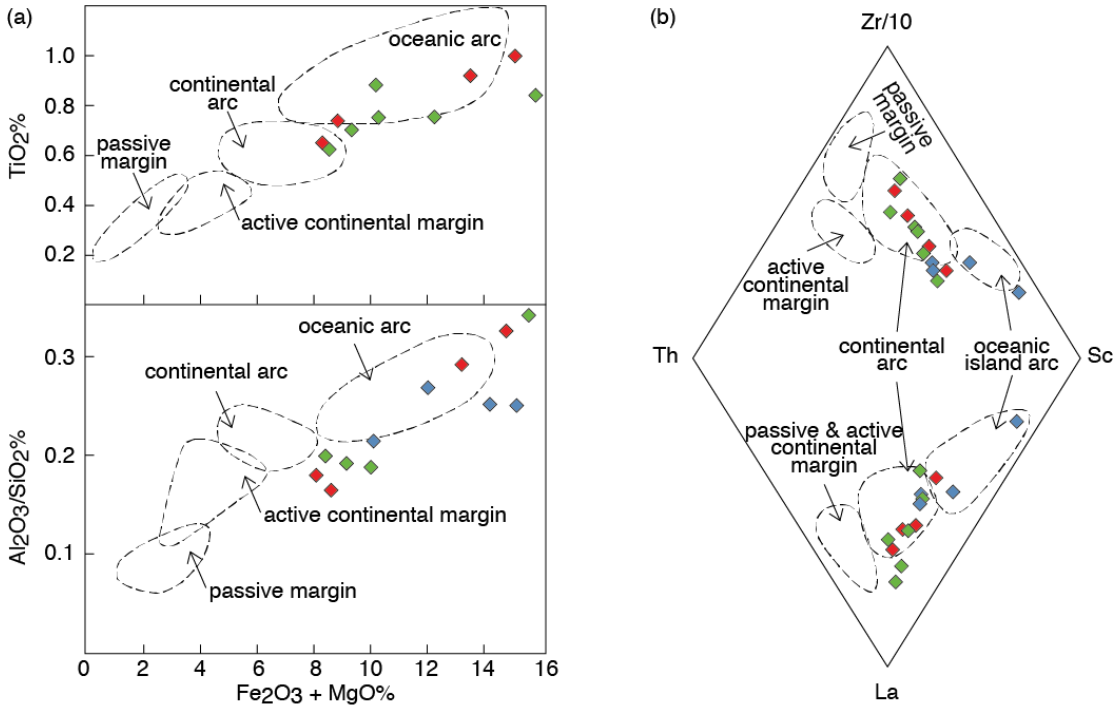

Fig. 14. Sedimentary samples from the Rombaksbotten, Gautelisvann and Ruvssot areas plotted on: (a) selected published discrimination diagrams emphasizing major element chemical variations (after

Bhatia, 1983); and (b) Sc-Th-Zr/10 discriminant plots (after Bhatia and Crook, 1986). These plots suggest that the sandstone was deposited in a continental island arc to oceanic arc tectonic setting. Symbol legend is the same as Fig. 9

A good tracer for mafic source components is the compatible element Sc, particularly when compared with Th, which is incompatible and enriched in felsic rocks. Both elements are generally immobile under surface conditions and therefore preserve the characteristics of their source, making the Th/Sc ratio a robust provenance indicator (Taylor and McLennan, 1985; McLennan et al., 1990). In sandstone from the study area, the Th/Sc ratios increase from 0.08 for sample ES131ac from Ruvssot to 0.92 for sample ES068.4R from RTW (Fig. 15a), whereas the Th/Sc ratio for the average upper continental crust is 0.79 (McLennan, 2001). The Th/Sc and Zr/Sc ratios can reveal compositional heterogeneity in provenances for the sandstone, if the samples show Th/Sc and Zr/Sc values along the trend from mantle to upper continental crust compositions (McLennan et al., 1993). The Zr/Sc ratio is commonly used as a measure of the degree of sediment recycling leading to the concentration of zircon in sedimentary rocks (McLennan, 1989; McLennan et al., 1993). Such a trend is present in Fig. 15a, suggesting input from a less evolved provenance.

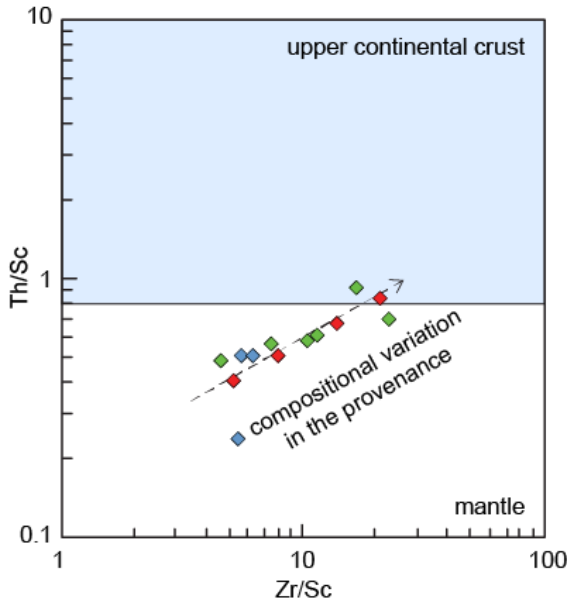

Fig. 15. Plot of turbiditic sandstone (greywacke) from the Rombaksbotten, Gautelisvann and Ruvssot areas on a Th/Sc versus Zr/Sc diagram (after McLennan et al., 1993), suggesting that the samples are sourced from 'primitive' material.

6.2. Tectonic setting for the mafic and ultramafic rocks

Most of the plots in Fig. 16 suggest mid-ocean ridge or arc affinities for the mafic and ultramafic units, which is similar to the continental- to island-arc tectonic setting for deposition of sandstone and shale units (discussed above). These similarities strengthen the suggestion that both the sedimentary and igneous rocks were emplaced during similar tectonic settings (~1900 Ma).

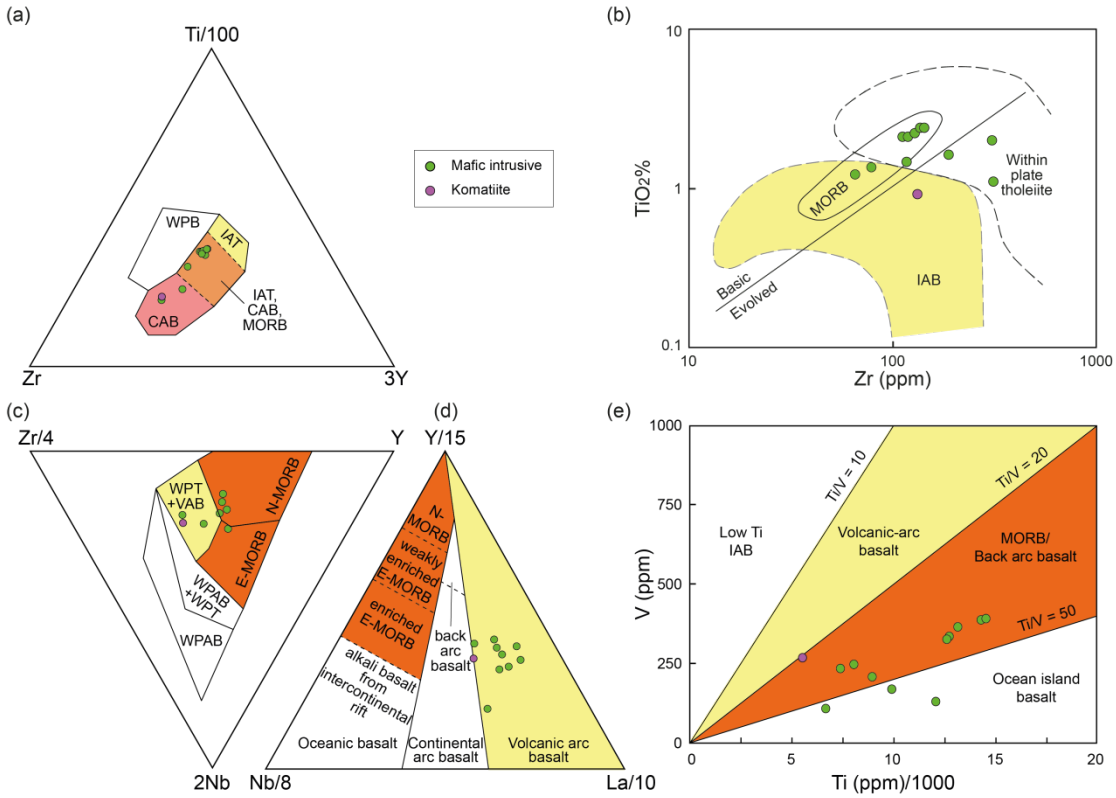

Fig. 16. Discriminations diagrams for mafic and ultramafic units plotted on: (a) Ti-Zr-Y diagram of Pearce and Cann (1973); (b) Ti–Zr diagram of Pearce (1982); (c) Nb–Zr–Y diagram of Meschede (1986); (d) La–Y–Nb diagram after Cabanis and Lecolle (1989); and (e) Ti–V diagram of Shervais (1982). These plots suggest that the mafic and ultramafic units have a mid-ocean ridge to volcanic arc setting.

6.3. Tectonic setting for the granitic rocks

On tectonic discriminant plots (Fig. 17), it is apparent that the granitic rocks in the RTW do not show a clear affinity towards a single, clearly isolated tectonic environment. Instead, they tend to overlap the boundaries of within plate and volcanic-arc granites, with most of the granites from Gautelisvann having a volcanic-arc affinity and most from Norddalen having a within-plate affinity (Fig. 17a, b). If we consider the R2 versus R1 discrimination plot of Batchelor and Bowden (1985), the granites can be interpreted predominantly as late orogenic granites (Fig. 17c).

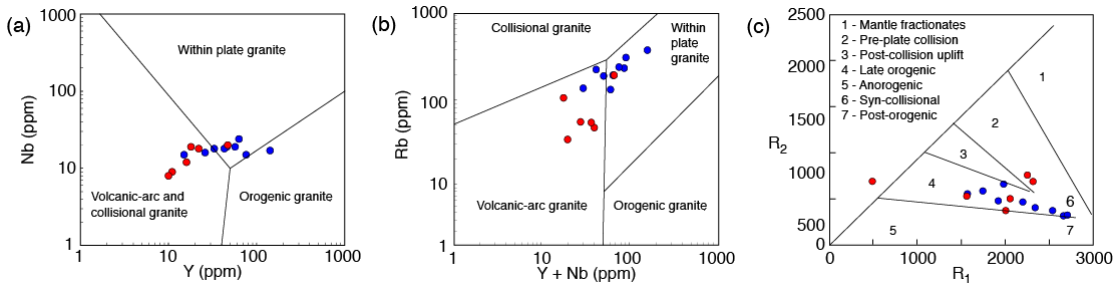

Fig. 17. Tectonic discrimination diagrams for of granites in the Rombak Tectonic Window: (a) Nb versus Y of Pearce et al. (1984); (b) Th/Yb versus Ta/Yb plot (after Pearce, 1982); and (c) R2 versus R1 of Batchelor and Bowden (1985; R1 = 4Si − 11(Na + K) − 2(Fe + Ti) and R2 = 6Ca + 2Mg + Al). Symbol legend same as in Fig. 10.

6.4. Progressive tectonic setting

On the primitive mantle plots of McDonough et al. (1992), which are normalized to the average greywacke composition in RTW (Fig. 18), the volcanic rocks, greywackes, granites, felsic and mafic intrusive rocks in the inlier plot in similar positions. In detail, the greywacke samples from Ruvsott and Rombaksbotten plot in similar positions as the mafic intrusives and intermediate volcanic rocks. Greywacke from Gautelisvann plots in a similar position as the tonalite and the felsic volcanic rock plots close to that of the granite from Gautelisvann. These similarities of the greywacke samples with the mafic and intermediate intrusions and volcanics suggest that they have developed in a similar tectonic setting and that the mafic intrusions and intermediate volcanic rocks are probable sources for the greywackes at Ruvsott and Rombaksbotten. Similarly, the greywacke samples from Gautelisvann plot in essentially the same positions as the underlying tonalite in Fig. 18, suggesting that the tonalite is a possible provenance for the greywacke in that location. Also the likeness of the felsic volcanic samples and the granite suggest that they may have developed from the same magma chamber, which is in accordance to what was suggested by

Korneliussen and Sawyer (1989). The mafic volcanic samples do not show similarities to any of the rocks in the area and suggest that they are either different magma chamber or not a source for the sedimentation of the studied rocks.

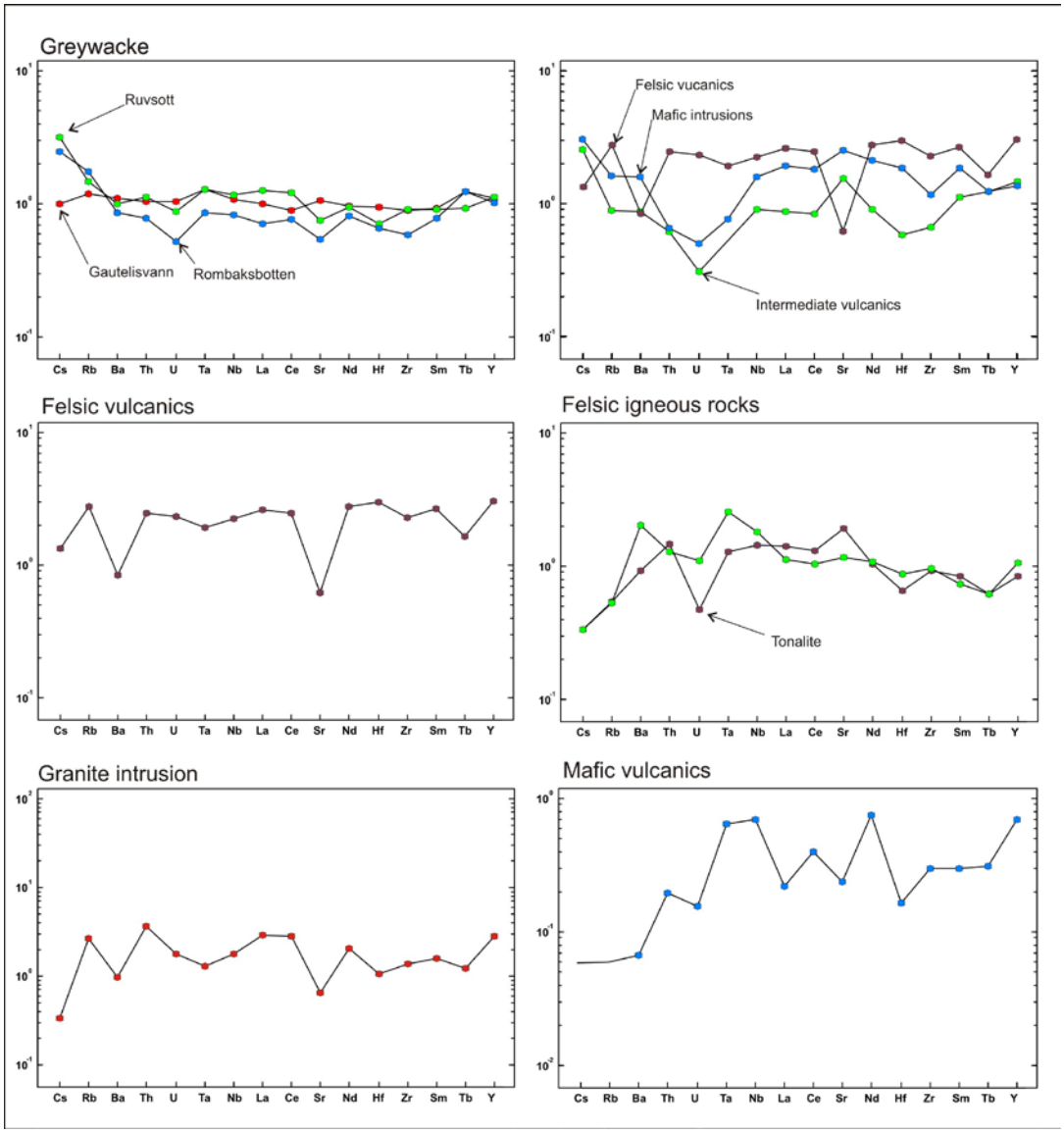

Fig. 18. Primitive mantle plots normalized to the average greywackes in the Rombak Tectonic Window (McDonough et al., 1992): a) the average of the metagreywacke from Rombaksbotten, Ruvsott and Gautelisvann; b) a plot showing the difference between the mean value from the felsic volcanic, intermediate volcanic and the mafic intrusions; c) the average of the felsic volcanic with high similarities to the average plot of the granite intrusions (e); d) the mean value of felsic igneous rocks and the tonalite rocks from Gautelisvann; e) the average of granite intrusion; and f) The average of the

mafic volcanic from Ruvsott that are different to the plots of felsic and intermediate volcanics. The diagrams are plotted based on the average of each category and shows the similarities between the metasedimentary rocks to the volcanic rocks and granites in the area.

7. Discussion and conclusions

The ca. 2000 – 1867 Ma metamorphosed greywacke and shale from RTW show some degree of variation from the east to the west, but in general, all samples plot within an active continental margin or island arc settings on discrimination diagrams (Fig. 3).

When the data is plotted in discrimination diagrams for clastic sediments, the plots for the sedimentary rocks vary with the sample location. For example, Fig. 3 (after Bhatia et al., 1983) shows that the samples from Ruvsott plot in an ocean arc field. The more westward located samples at Rombaksbotten and Gautelisvann plot on a line from oceanic arc to a continental-arc setting (Fig. 3). Similarly, the chemical variation diagram show that there are mafic and intermediate provenances for the metasedimentary rocks and that the samples taken from the east have an increased mafic (basaltic) provenance than those from the west, which appear to have an andesite provenance. Furthermore, the plot in Fig. 15 indicates that the felsic volcanic rocks are sourced largely from a primitive (mantle) source.

Therefore, based on the discrimination plots (Fig. 14), we suggest that the metasedimentary rocks in the RTW were deposited in an island arc to active continental margin setting, from a provenance dominated by mafic to intermediate compositions. A possible source could be erosion of the ~1900 Ma mafic to felsic volcanic rocks found in the study area.

The ca. 2000 – 1867 Ma mafic and ultramafic rocks in the RTW plot predominantly in the continental to oceanic arc fields of Fig. 14. This is consistent

with the proposed island-arc to active continental margin setting for the sedimentary units discussed above, which confirms that these settings are probably valid for both the sedimentary and volcanic rocks in the RTW.

The ca. 1790 Ma felsic intrusive rocks can be classified as I-type or partially fractionated A-type granites (Fig. 12). These rocks plot in the late-orogenic to anorogenic fields associated with a volcanic-arc to within-plate tectonic setting (Figs. 12c and 17), which is not too dissimilar from that for the ca. 1900 Ma metasedimentary and volcanic units. This suggests that the granites intruded these metamorphosed sedimentary and volcanic rocks during accretion associated with the Svecofennian Orogeny.

The Na_2O+K_2O enrichment of A-type granitic rocks was also taken as a fundamental diagnostic parameter by Collins et al. (1982) and Whalen et al. (1987), who stressed other characteristics of such rocks. Other factors include high contents of Zr, Nb, W, Mo, REE, and the Ga:Al ratio. Pitcher (1983) and Brown et al. (1984) consider A-type granites to be related to alkaline and peralkaline monzogranites, granodiorites and syenites. Data presented by several researchers during the last decades indicate that most of these rocks are formed in late- to post-collisional settings (Harris et al., 1986; Sylvester, 1989; Bonin, 1990, 2007; Bitencourt and Nardi, 2000).

Because of the similarities in the geochemical characteristics of the rocks in RTW, we suggest these rocks developed in a progressive tectonic event starting with an island-arc setting for the mafic intrusions and intermediate volcanic rocks deposited over tonalite. The mafic and volcanic rocks were subsequently the provenance for the turbidite units at Ruvsott and Rombaksbotten, and the mafic intrusive, intermediate

volcanics and tonalite are the provenance for the turbidite units at Gautelisvann. The tectonic setting progressed into a continental-arc setting with deposition of felsic volcanic units and the emplacement of granites during ca. 1820-1790 Ma. These successions were then accreted on to the Baltic continent. The tectonic setting for the Paleoproterozoic is here schematically summarized in Fig. 19, which covers a ~70 million year period.

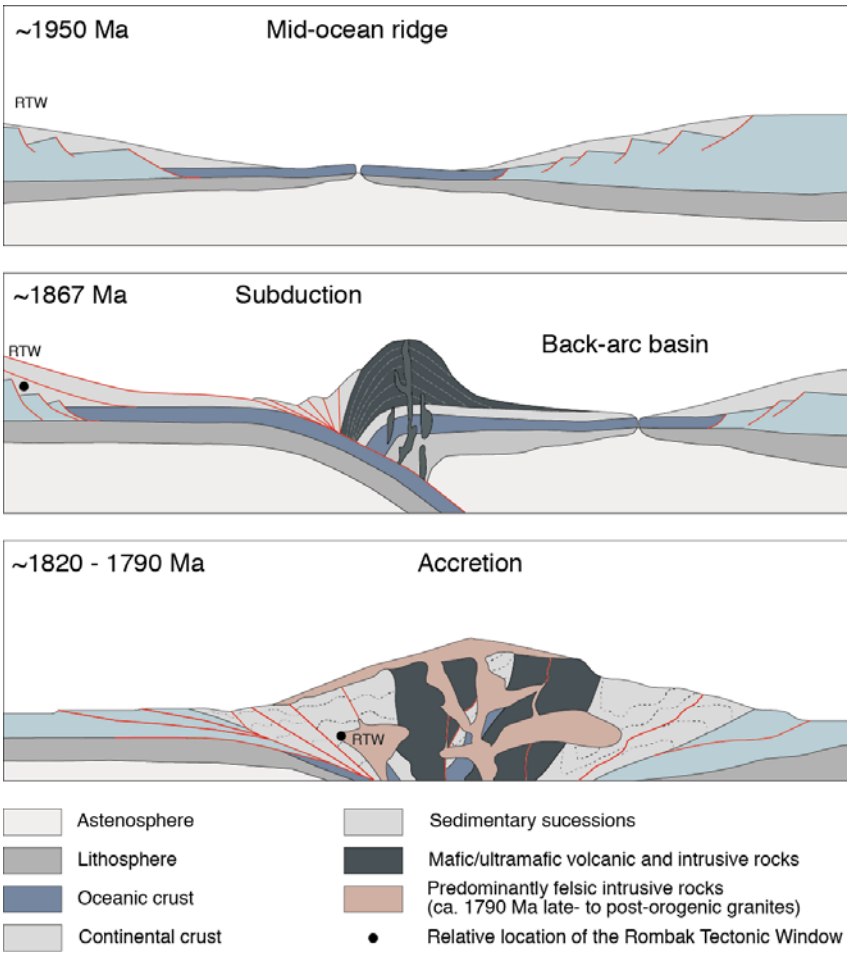

Fig. 19. Model for the tectonic setting during deposition of the ca. 2000 – 1867 Ma sedimentary and volcanic rocks in the Rombak Tectonic Window.

Acknowledgements

This contribution is part of the Rombaken and Skjomen project in northern Norway by the Geological Survey of Norway and University of Tromsø. We also acknowledge the Australian Research Council (ARC) Linkage Project LP110100667 and the ARC Centre of Excellence for Core to Crust Fluid Systems (CCFS). The constructive comments from Iain Henderson have significantly improved this manuscript.

References

Armstrong, R.L., Harmon, R.S., 1981. Radiogenic Isotopes: The Case for Crustal Recycling on a Near-Steady-State No-Continental-Growth Earth. Transactions of the Royal Society of London A301, 443–472.

Bargel, T.H., Bergstrøm, B., Boyd, R., Karlsen, T.A., 1995. Geologisk kart, Narvik kommune M 1:100.000: Norges geologiske undersøkelse.

Barton, M.D., Young, S., 2002. Non-pegmatitic deposits of beryllium: mineralogy, phase equilibria and origin. Reviews in Mineralogy and Geochemistry 50, 591–691.

Batchelor, R.A., Bowden, P., 1985. Petrogenetic interpretation of granitoid rock series using multicationic parameters. Chemical Geology 48, 43–55.

Bergh et al., 2010. Neoarchaean to Svecofennian tectono-magmatic evolution of the West Troms Basement Complex, North Norway. Norwegian Journal of Geology, 90, 21-48.

Berthelsen, A., Marker, M., 1986. 1.9-1.8 Ga old strike-slip megashear in the Baltic Shield, and their plate tectonic implications. Tectonophysics 128, 163–181.

Bevins, R.E., Kokelaar, B.P., Dunkley, P.N., 1984. Petrology and geochemistry of lower to middle Ordovician igneous rocks in Wales: a volcanic arc to marginal basin transition. Proceedings of the Geologists' Association 95, 337–347.

Bhatia, M.R., 1983. Plate tectonics and geochemical composition of sandstones. J. Geol. 91, 611–627.

Bhatia, M.R., 1985a. Composition and classification of Paleozoic flysch mudrocks of eastern Australia: implications in provenance and tectonic setting interpretation. Sed. Geol. 41, 249–268.

Bhatia, M.R., 1985b. Rare earth element geochemistry of Australian Paleozoic sandstones and mudrocks: provenance and tectonic control. Sed. Geol. 45, 97–113.

Bhatia, M.R., Crook, K.A.W., 1986. Trace elements characteristics of graywakes and tectonic setting discrimination of sedimentary basins. Contrib. Mineral. Petrol. 92, 181–193.

Bhatia, M.R., 1983. Plate tectonics and geochemical composition of sandstones. J. Geol. 91, 611–627.

Bhatia, M.R., Crook, K.A.W., 1986. Trace elements characteristics of graywakes and tectonic setting discrimination of sedimentary basins. Contrib. Mineral. Petrol. 92, 181–193.

Bitencourt, M.F., Nardi, L.V.S., 2000. Tectonic setting and sources of magmatism related to the Southern Brazilian Shear Belt. Revista Brasileira de Geociências 30, 184–187.

Bonin, B., 1990. From orogenic to anorogenic settings: evolution of granitoid suites after a major orogenesis. Geological Journal 25, 261–270.

Bonin, B., 2007. A-type granites and related rocks: evolution of a concept, problems and prospects. Lithos 97, 1–29.

Braathen, A., Davidsen, B., 2000. Structure and stratigraphy of the Paleoproterozoic Karasjok Greenstone Belt, north Norway – regional implications. Norsk Geologisk Tidsskrift 80, 33-50.

Brown, G.C., Thorpe, R.S., Webb, P.C., 1984. The geochemical characteristics of granitoids in contrasting arcs and comments on magma sources. Journal of the Geological Society London 141, 413–426.

Cabanis, B., Lecolle, M., 1989. Le diagramme La/10 -Y/15 -Nb/8: Un outil pour la discrimination des series volcaniques et la mise en evidence des procesus de melange et/ou de contamination crutale. Comptes Rendus de l'Académie des Sciences 309, 2023–2029.

Chappell, B.W., White, A.J.R., 1974. Two contrasting granite types. Pacific Geology 8, 173–174.

Coller, D., 2004. Varden Ridge Target Generation Report: Golden Chalice Resources Inc report, v. GT 04-18D-01.

Collins, W.J., Beams, S.D., White, A.J.R., Chappell, B.W., 1982. Nature and origin of A-type granites with particular reference to southeastern Australia. Contributions to Mineralogy and Petrology 80, 189–200.

Compston, W., Williams, I. S., Meyer, C., 1984. U–Pb geochronology of zircons from lunar breccia 73217 using a sensitive high mass-resolution ion microprobe. Journal of Geophysical Research 89, B252–B534.

Cox, K.G., Bell, J.D., Pankhurst, R.J., 1979. The interpretation of igneous rocks. George, Allen and Unwin, London, 464 pp.

Cullers, R.L., Barrett, T., Carlson, R., Robinson, B., 1987. Rare earth element and mineralogic changes in Holocene soil and stream sediment: a case study in the Wet Mountains, Colorado, USA. Chem. Geol. 63, 275–297.

de la Roche, H., Leterrier, J., Grandclaude, P., Marchal, M., 1980. A classification of volcanic and plutonic rocks using R1R2-diagram and major-element analyses: Its relationships with current nomenclature. Chemical Geology 29(1–4), 183–210.

Drake, M.J., Weill, D.F., 1975. Partition of Sr, Ba, Ca, Y, Eu2+, Eu3+, and other REE between plagioclase feldspar and magmatic liquid: an experimental study. Geochimica et Cosmochimica Acta 39, 689–712.

Eggins, S. M., Woodhead, J. D., Kinsley, L. P. J., Mortimer, G. E., Sylvester, P., McCulloch, M. T., Hergt, J. M., Handler, M. R., 1997. A simple method for the precise determination of >40 trace elements in geological samples by ICPMS using enriched isotope internal standardisation. Chemical Geology 134, 311–326.

Fossen, H., 2000. Extensional tectonics in the Caledonides: synorogenic or postorogenic? Tectonics 19, 213-224.

Frost, B.R., Barnes, C.G., Collins, W.J., Arculus, R.J., Ellis, D.J., Frost, C.D., 2001. A geochemical classification for granitic rocks. Journal of Petrology 42, 2033–2048.

Gaál, G., Gorbatschev, R., 1987. An outline of Precambrian evolution of the Baltic Shield. Precambrian Research 35, 15–52.

Gorbatschev, R., 1985. Precambrian basement of the Scandinavian Caledonides. In: Gee, D.G., Sturt, B.A. (Eds.), The Caledonide Orogen-Scandinavia and Related Areas. Wiley, Chichester, pp. 197–212.

Gromet, L.P., Dymek, R.F., Haskin, L.A., Korotev, R.L., 1984. The ‘North American Shale Composite’: its compilation, major and trace element characteristics. Geochimica et Cosmochimica Acta 48, 2469–2482.

Gustavson, M., Gjelle, S.T., 1991. Geological Map of Norway (1:250 000) Mo i Rana. Geological Survey of Norway.

Harris, N.W.B., Pearce, J.A., Tindle, A.G., 1986. Geochemical characteristics of collision-zone magmatism. In Coward, M.P., Ries, A.C. (Eds.), Collision Tectonics. Geological Society Special Paper 19, 115–158.

Henderson, I.H.C., Kendrick, M., 2003. Structural controls on graphite mineralisation, Senja, Troms. Geological Survey of Norway Report 2003.011, 16pp.

Henderson, I.H.C., Viola, G., 2013. Structural analysis of the Kautokeino Greenstone Belt from geophysical and field studies: Towards a refined understanding of its gold mineralisation. Proceedings of the Geological Society of Norway, Winter Conference, Oslo.

Hietanen, A., 1975. Generation of potassium-poor magmas in the northern Sierra Nevada and the Svecofennian in Finland. Journal of Resources U.S. Geological Survey 3(6), 631-645.

Harker, A., 1909. The natural history of igneous rocks. Methuen, London.

Irvine, T.N., Baragar, W.R.A., 1971. A guide to the chemical classification of the common volcanic rocks. Canadian Journal of Earth Science 8, 523–548.

Kärki A., Laajoki, K., 1995. An interlinked system of folds and ductile shear zones – late stage Svecokarelian deformation in the central Fennoscandian Shield, Finland. Journal of Structural Geology 17, 1233–1247.

Klein, A.C., Steltenpohl, M.G., Hames, W.E., Andresen, A., 1999. Ductile and brittle extension in the southern Lofoten Archipelago, northern Norway: implications for differences in tectonic style along an ancient collision margin. American Journal of Science 299, 69–89.

Korja, A., Lahtinen, R., Nironen, M., 2006. The Svecofennian orogen: a collage of microcontinents and island arcs, *in* Gee, D.G., Stephenson, R.A. (Eds.), European Lithosphere Dynamics. Geological Society, London, Memoirs 32, 561-578.

Korneliussen, A., Tollefsrud, J.I., Flood, B., Sawyer, E., 1986. Precambrian volcano-sedimentary sequences and related ore deposits, with special reference to the Gautelisfjell carbonate-hosted gold deposit, Rombaken basement window, Northern Norway. Geological Survey of Norway Report 86.193, 44p.

Korneliussen, A. and Sawyer, E. W. (1989). The geochemistry of Lower Proterozoic mafic to felsic igneous rocks, Rombak Window, North Norway. NGU Bulletin 415: 7-21.

Kuno, H., 1968. Differentiation of basalt magmas. In: Hess, H.H., Poldervaart, A. (Eds.), Basalts, the Poldervaart treatise on rocks of basaltic composition, vol. 2. Wiley and Sons, New York, p. 623-688.

Lahtinen, R., Garde, A.A., Melezhik, V.A., 2008. Paleoproterozoic evolution of Fennoscandia and Greenland. Episodes 31, 20-28.

Larsen, T., Bergh, S.G., Henderson, I.H.C., Korneliussen, A., Kullerud, K., 2010. Svecofennian structural development and metallogenesis of Paleoproterozoic volcano-sedimentary rocks of Rombak Tectonic widow: NGF abstract proceedings of the Geological Society of Norway, v. 1, 29th Nordic Geological winter meeting, Oslo.

Larsen, T., Sundblad, K., Henderson, I.H.C., Bergh, S.G., Bagas, L., Sandstad, J.S., Andersen, T., and Simonsen, S., 2013. Recognition of Svecofennian sulphide bearing crust in the Rombak region, northern Norway: NGF abstract proceedings of the Geological Society of Norway, v. 1, 32nd Nordic Geological winter meeting, Oslo.

Lesher, C.M., Gibson, H.L., Campbell, I.H., 1986. Composition-volume changes during hydrothermal alteration of andesite at Buttercup Hill, Noranda District, Quebec. Geochimica et Cosmochimica Acta 50, 2693–2705.

Lindh, A., 1987. Westward growth of the Baltic Shield. Precambrian Research 35, 53-70.

Ludwig, K. R., 2003. Isoplot/Ex version 3: A Geochronological Toolkit for Microsoft Excel, User's Manual. Berkeley Geochronology Center Special Publications 4, 70 p.

Ludwig, K. R., 2009. SQUID 2: A User's Manual. Berkeley Geochronology Center Special Publication 5, 110p.

Lundqvist, Th., 1987. Early Svecofennian stratigraphy of southern and central Norrland, Sweden, and possible existence of an Archaean basement west of the Svecokarelides. Precambrian Research 35, 343-352.

McCarthy, T.S., Hasty, R.A., 1976. Trace element distribution patterns and their relationship to the crystallization of granitic melts. Geochimica et Cosmochimica Acta 40, 1351–1358.

McDonough, W.F., Sun, S.-S., Ringwood, A.E., Jagoutz, E., Hofmann, A.W., 1992)\. Potassium, Rubidium and Cesium in the Earth and Moon and the evolution of the mantle of the Earth. Geochimica et Cosmochimica Acta 56, 1001–1012.

McLennan, S.M., 1989. Rare earth elements in sedimentary rocks: Influence of provenance and sedimentary process. Mineral. Soc. Am. Rev. Mineral. 21, 169–200.

McLennan, S.M., 2001. Relationships between the trace element composition of sedimentary rocks and upper continental crust. Geochem. Geophys. Geosyst. 2, 2000GC000109.

McLennan, S.M., Hemming, S., McDaniel, D.K., Hanson, G.N., 1993. Geochemical approaches to sedimentation, provenance, and tectonics. Geol. Soc. Am. Special Paper 284, 21–40.

McLennan, S.M., Taylor, S.R., McCulloch, M.T., Maynard, J.B., 1990. Geochemical and isotopic determination of deep sea turbidites: Crustal evolution and plate tectonic associations. Geochim. Cosmochim. Acta 54, 2015–2049.

Meschede, M., 1986. A method of discriminating between different types of mid-ocean ridge basalts and continental tholeiites with the Nb–Zr–Y diagram. Chemical Geology 83, 55–69

Moorbath, S., 1977. Ages, isotopes and evolution of Precambrian continental crust. Chemical Geology 20, 151-–187.

Myers, J.S., Kroner, A. 1994. Archaean tectonics. In: Hancock, P.L. (Ed.), Continental Deformation. Pergamon Press, Oxford.

Myhre, P.I., Corfu, F.C., Bergh, S., 2011. Paleoproterozoic (2.0–1.95 Ga) pre-orogenic supracrustal sequences in the West Troms Basement Complex, North Norway. Precambrian Research 186(1-4), 89-100.

Nesbitt, H.W., Young, G.M., 1989. Formation and diagenesis of weathering profiles. Journal of Geology 97, 129–147.

Nironen, M., 1997. The Svecofennian Orogen: a tectonic model. Precambrian Research 86, 21–44.

Norrish, K., Chappell, B.W., 1997. X-ray fluorescence spectrometry. In: Zussman, J. (Ed.), Physical Methods in Determinative Mineralogy, 2nd Edition. Academic Press, London, pp.201–272.

Norrish, K., Hutton, J.T., 1969. An accurate X-ray spectrographic method for the analysis of a wide range of geological samples. Geochim Cosmochim Acta 33, 431–453.

Olesen, O., Sandstad, J.S., 1993. Interpretation of the Proterozoic Kautokeino Greenstone Belt, Finnmark, Norway, from combined geophysical and geological data. Geological Survey of Norway Bulletin 425, 43–62.

Pearce, J.A., Cann, J.R., 1973. Tectonic setting of basic volcanic rocks determined using trace element analysis. Earth and Planetary Science Letters 19, 290–300.

Pearce, J.A., 1982. Trace element characteristics of lavas from destructive plate boundaries. In: Thorpe, R.S. (Ed.), Andesites. Wiley, New York, pp. 525–528.

Pearce, J.A., Harris, N.B.W., Tindle, A.G., 1984. Trace element discrimination diagrams for the tectonic interpretation of granitic rocks. Journal of Petrology 25, 956–983.

Peccerillo, A., Taylor, S.R., 1976. Geochemistry of Eocene calcalkaline volcanic rocks from the Kastamonu area, Northern Turkey. Contributions to Mineralogy and Petrology 58, 68–81.

Pidgeon, R.T., Furfaro, D., Kennedy, A. K., Nemchin, A.A., Van Bronswijk, W., 1994. Calibration of zircon standards for the Curtin SHRIMP II, *in* Eighth International Conference on Geochronology, Cosmochronology, and Isotope Geology - Abstracts. U.S. Geological Survey Circular 1107, p. 251.

Pitcher, W.S., 1983. Granite: typology, geological environment and melting relationships. In Atherton, M.P., Gribble, C.D. (Eds.), Migmatites, Melting and Metamorphism. Shiva Publishing Limited, Cheshire, U.K., p. 277–287.

Pyke, J., 2000. Mineral laboratory staff develops new ICP-MS preparation method. Australian Geological Survey Organisation Newsletter 333, 12–14.

Rollinson, H., 1996. Using Geochemical Data: Evaluation, Presentation, Interpretation. Longman Geochemistry Series, p. 75-76.

Rudnick, R., Gao, S., 2004. Composition of the continental crust. In: Holland, H.D., Turekian, K.K. (Eds.), Treatise on Geochemistry, Vol. 3. Elsevier, Amsterdam, pp. 1–64.

Sawyer, E., 1986. Metamorphic assemblages and conditions in the Rombak Basement Window. Geological Survey of Norway Report 86.168, 25pp.

Sawyer, E. W. and Korneliussen, A. (1989). The geochemistry of Lower Siliciclastic turbidites from the Rombak Window: implications for palaeogeography and tectonic settings. NGU Bulletin 415: 23-38.

Schandl, E.S., Gorton, M.P., Wateneys, H.A., 1995. Rare earth element geochemistry of the metamorphosed volcanogenic massive sulphide deposits of the Manitouwadge mining camp, Superior province, Canada: a potential exploration tool? Economic Geology 90, 1217–1236.

Stern, RA 2001, A new isotopic and trace-element standard for the ion microprobe: preliminary thermal ionization mass spectrometry (TIMS) U–Pb and electron-microprobe data: Geological Survey of Canada, Radiogenic Age and Isotopic Studies, Report 14, Current Research 2001-F1, 11p.

Stern, R. A., 2009. Measurement of SIMS instrumental mass fractionation of Pb isotopes during zircon dating. Geostandards and Geoanalytical Research 33(2), 145-168.

Shervais, J.W., 1982. Ti–V plots and the petrogenesis of modern and ophiolitic lavas. Earth and Planetary Science Letters 59, 101–118.

Sylvester, P.J., 1989. Post-collisional alkaline granites. Journal of Geology 97, 261–280.

Taylor, S.R., McLennan, S.M., 1985. The continental crust: its composition and evolution. Blackwell, Oxford, 312 pp.

Taylor, S.R., McLennan, S.M., Armstrong, R.L., Tarney, J., 1981. The Composition and Evolution of the Continental Crust: Rare Earth Element Evidence from Sedimentary Rocks. Philosophical Transactions of the Royal Society of London A301, 381–399.

Weaver, B.L., Tarney, J., 1984. Empirical approach to estimating the composition of the continental crust. Nature 310, 575–577.

Welin, E., Christansson, K., Kähr, A.-M. , 1993. Isotopic investigations of metasedimentary and igneous rocks in the Paleoproterozoic Bothnian Basin, central Sweden. Geologiska Föreningen i Stockholm Förhandlingar 115(4), 285-296.

Whalen, J.B., Currie, K.L., Chappell, B.W., 1987. A-type granites: geochemical characteristics, discrimination and petrogenesis. Contributions to Mineralogy and Petrology 95, 407–419.

White, A.J.R., Chappell, B.W., 1983. Granitoid types and their distribution in the Lachlan Fold Belt, southeastern Australia. Geological Society of America Memoir 159, 21–34.

White, A.J.R., Chappell, B.W., 1988. Some supracrustal (S-type) granites of the Lachlan Fold Belt. Transactions of the Royal Society of Edinburgh: Earth Sciences 79, 169–181.

Whitehead, D., 2010, Moraine as a Source of Gold in Stream Sediments and the Relationship to a Shear Zone in the Rombak-Skjomen Area of Norway: Master thesis from Luleå University of Technology, Department of Chemical Engineering and Geosciences.

Wilson, M., 1989. Igneous Petrogenesis: A Global Tectonic Approach. Chapman and Hall, London, UK, 465 pp.

Wimmenauer, W., 1984. Das prävaristische Kristallin im Schwarzwald. Fortschr. Miner. Beih. 62, 69–86.

Appendix

A-1. Geochemistry of greywacke and shale units (Sawyer and Korneliussen, 1989).

Id	SiO2	Al2O3	Fe2O3	FeO	TiO2	CaO	MgO	Na2O	K2O	MnO	P2O5	V	Sc	Co	Cr	Ni	Cu	Zn	Pb	Rb	Sr	Ba	Zr	Y	Nb	Cs	Th	U	Ta	Hf	La	Ce	Nd	Sm	Eu	Tb	Yb	Area
ES057.4G	71,35	11,68	0,63	5,66	0,73	2,67	2,33	2,27	1,80	0,06	0,13	137	12		262	46	84	111		75	231	778	252	20	8	2	10	3	1	6	36	74	25	5	1	1	2	Gautelisvann
ES058.4G	70,48	12,56	0,58	5,21	0,65	2,77	2,41	2,49	1,86	0,06	0,13	118	12		187	54	51	111		77	246	622	167	18	9	3	8	3	1	4	25	52	22	4	1	1	2	Gautelisvann
ES060.4G	57,84	16,78	0,93	8,32	0,93	2,78	4,27	3,23	3,45	0,09	0,12	223	18		229	116		190		133	285	959	143	26	12						32	39						Gautelisvann
ES061.4G	54,62	17,69	1,03	9,22	1,00	2,85	4,64	3,59	3,89	0,09	0,12	279	25		266	135	6	144		126	291	981	130	24	14	4	10	4	1	3	22	50	19	4	1	1	3	Gautelisvann
ES067.4R	66,46	14,13	0,70	6,28	0,75	1,45	3,28	3,01	2,71	0,06	0,13	144	15		245	75	6	103		110	149	704	173	24	12						52	91						Rombaksbotten
ES068.4R	68,98	13,14	0,62	5,59	0,70	1,06	2,99	3,48	2,42	0,05	0,12	131	12		301	72	11	82		88	173	873	201	25	11	5	11	283	1	5	33	77	28	5	1	1	2	Rombaksbotten
ES072.4R	68,80	13,62	0,57	5,13	0,62	2,30	2,77	3,08	2,26	0,05	0,11	112	14		215	67	59	86		105	247	697	147	15	8	7	8	3	1	3	28	59	23	4	1	-	2	Rombaksbotten
ES073.4R	68,09	12,72	0,70	6,31	0,88	1,84	3,06	2,89	2,58	0,07	0,15	155	13		387	63	35	91		102	168	775	297	30	11						61	109						Rombaksbotten
ES069.4R	53,44	18,15	1,05	9,40	0,84	2,41	5,35	3,41	4,19	0,08	0,13	198	23		212	124	109	147		205	227	598	106	18	17	14	11	3	1	2	29	62	24	5	1	1	2	Rombaksbotten
ES070.4R	60,73	16,22	0,81	7,24	0,76	1,07	4,24	3,63	3,76	0,07	0,11	158	18		210	82	18	23		151	155	876	134	22	11	12	10	3	1	3	16	37	10	3	1	1	2	Rombaksbotten
ES131AC	51,96	13,42	1,29	11,56	1,27	6,01	8,69	2,98	1,80	0,13	0,12	254	37	43	503	211	84	132	13	66	157	785	103	28	9	6	3	1	-	2	11	26	12	3	1	1	2	Ruvssot
ES132AC	56,31	14,04	1,12	10,03	0,85	1,59	6,78	2,56	5,30	0,09	0,15	141	20	35	332	139	67	62	9	190	118	660	112	19	7	8	10	2	1	3	24	51	19	4	1	1	1	Ruvssot
ES133C	58,45	14,54	0,96	8,66	0,90	1,99	5,65	3,57	4,36	0,08	0,13	128	21	30	279	109	76	47	10	161	153	429	114	16	9		5			4	0	50						Ruvssot
ES134AC	58,55	14,66	0,98	8,79	0,88	2,87	4,62	2,72	4,80	0,09	0,13	132	20	28	228	98	12	48	12	191	112	726	125	18	8	8	10	2	1	3	27	58	24	4	1	1	2	Ruvssot

A-2. Geochemistry of mafic and ultramafic rocks (Korneliussen and Sawyer, 1989)

Id	SiO2	Al2O3	Fe2O3	TiO2	CaO	MgO	Na2O	K2O	MnO	P2O5	V	Sc	Co	Cr	Ni	Cu	Zn	Pb	Rb	Sr	Ba	Zr	Y	Nb	Cs	Th	U	Ta	Hf	La	Ce	Nd	Sm	Eu	Tb	Yb	Area
G2.4GB	48,12	13,41	15,31	2,19	8,97	5,37	2,30	1,35	0,22	0,77	365	36	42	48	45	59	160	15	36	382	846	128	38	8						27	54						Gautelisvann
G4.4GB	47,60	15,99	12,59	1,23	9,81	7,55	1,90	1,05	0,18	0,34	234	28	62	103	121	65	127	13	39	392	433	65	20	6						13	19						Gautelisvann
G5.4GB	48,41	13,81	14,58	2,12	9,56	5,75	2,80	1,03	0,22	0,84	335	36	52	101	49	48	167	17	28	422	617	119	34							27	51						Gautelisvann
G6.4GB	48,75	12,51	16,12	2,38	8,74	4,84	2,60	1,53	0,23	0,95	387	33	41	18	30	49	222	14	43	371	872	137	38	7						40	72						Gautelisvann
G7.4GB	48,49	13,48	15,39	2,42	9,65	5,28	2,70	0,96	0,24	0,95	391	39	41	28	32	22	189	15	24	427	649	143	40	6						35	73						Gautelisvann
K133.4G	48,38	16,32	12,36	1,34	9,67	6,22	2,30	1,20	0,17	0,40	247	29	43	79	77	66	133	11	39	455	580	78	21	5	2	1	-	-	2	19	39	14	4	1	1	2	Gautelisvann
K071.85S	59,82	15,24	6,52	1,11	4,25	3,38	3,94	4,57	0,11	0,31	108	14	16	136	31	34	71	18	145	480	1220	309	25	20		18			5	46	99						Norddalen
K132A.4	53,28	15,63	12,73	2,21	4,16	4,39	1,10	3,37	0,13	0,43	401	27	38	45	38	152	137		151	207	715	192	37	10						40	68						Norddalen
K152.3GK2	47,79	13,53	14,71	2,10	9,21	5,58	2,70	1,37	0,20	0,83	326	34	38	103	55	23	120	15	55	397	574	112	34							32	65	37	9	2	1	2	Norddalen
K268.3N	50,50	14,94	12,19	1,49	8,88	6,25	2,50	1,45	0,18	0,35	208	31	42	134	31	15	142	16	64	387	483	116	26		2	2	1	-	3	25	52	21	5	1	1	2	Norddalen
K273.3N	55,27	14,29	10,83	1,65	6,15	4,26	2,70	3,04	0,15	0,62	169	20	34	91	24	13	131	20	144	378	938	186	40	13						44	88	44	10	2	1	3	Norddalen
K274.3N	57,46	13,80	11,17	2,01	5,09	2,26	3,40	2,98	0,15	0,89	130	18	22		6	10	143	16	86	332	1300	306	49	16						52	116						Norddalen
R001.3RT	48,57	9,88	13,04	1,30	6,86	7,75	4,10	0,17	0,09	0,12	213	21	36	277	90	11	38			107	56	93	13	6						14	25	16	3	1	-	1	Ruvssot
R004.3RT	48,81	9,63	10,05	0,92	6,20	21,04	2,50	0,12	0,13	0,10	268	24	74	550	234	16	43			107	80	132	21	8		6	1	1	3	16	23	18	4	1	1	2	Ruvssot
R016.3RT	47,40	6,92	8,74	0,20	6,70	28,76	0,01	0,01	0,18	0,02	154	27	55	3000	1400	45	46				42	21				-	-		-	0			-	-		1	Ruvssot
R022.3RT	45,55	7,49	10,63	0,25	8,85	20,56	0,50	0,03	0,16	0,02	168	26	89	2200	1 000	8	98			9	25	25	8			-		-	-	1			-	-	-	1	Ruvssot
R023.3RT	44,03	4,80	8,76	0,16	5,05	28,77	0,01	0,01	0,17	0,01	131	20	111	2600	1600	5	55			15	48	18				1				1						1	Ruvssot

Table A-3. Geochemistry of the ca. 1790 Ma felsic igneous rocks in the Rombak Tectonic Window (Korneliussen and Sawyer, 1989).

Id	SiO2	Al2O3	Fe2O3	TiO2	CaO	MgO	Na2O	K2O	MnO	P2O5	V	Sc	Co	Cr	Ni	Cu	Zn	Pb	Rb	Sr	Ba	Zr	Y	Nb	Th	U	Hf	La	Ce	Eu	Area
K142.85	60,55	18,49	4,49	0,67	2,03	2,19	8,54	1,53	0,05	0,19	63,00	9,00	7,00	22,00	15,00	3,00	43,00	16,00	47,00	353,00	361,00	206,00	22,00	18,00	13,00	2,33	2,00	43,00	79,00	0,50	Gautelisvann
ES083GR	66,04	15,26	4,87	0,64	2,25	0,96	3,40	5,53	0,06	0,18	43,00	8,00	11,00	13,00	6,00	8,00	81,00	20,00	197,00	234,00	1200,00	367,00	46,00	19,00	24,00	4,30	0,50	96,00	204,00	0,50	Norddalen
K063.85S	66,13	13,99	0,78	5,40	2,76	1,81	3,51	4,36	0,09	0,28	58,00	11,00	10,00	37,00	14,00	12,00	75,00	26,00	193,00	212,00	895,00	248,00	33,00	18,00	16,00	2,87	8,00	58,00	124,00	0,50	Norddalen
ES081GR	66,40	15,83	3,82	0,51	2,04	0,59	4,10	5,45	0,06	0,13	23,00	5,00	7,00	2,00		1,00	43,00	25,00	133,00	229,00	1300,00	352,00	43,00	18,00	28,00	6,00	9,00	127,00	233,00	2,00	Norddalen
K152.85	67,00	14,73	4,19	0,62	1,93	0,76	4,00	5,75	0,08	0,18	31,00	10,00	6,00	8,00	6,00	28,00	58,00	28,00	197,00	178,00	1008,00	270,00	47,00	20,00	15,00	2,69	3,00	65,00	132,00	0,50	Gautelisvann
K140.85	67,29	14,91	4,47	0,54	3,60	1,54	4,50	2,12	0,05	0,13	56,00	8,00	6,00	9,00	7,00	11,00	36,00	12,00	55,00	377,00	967,00	180,00	16,00	12,00	8,00	1,00	5,00	30,60	62,90	1,00	Gautelisvann
K144.85	69,25	14,95	3,13	0,44	3,21	1,01	4,92	1,94	0,06	0,12	34,00	8,00	3,00	7,00	8,00	2,00	31,00	12,00	54,00	692,00	722,00	219,00	18,00	19,00	19,00	3,41	2,00	45,00	89,00	0,50	Gautelisvann
K275.3N	69,37	13,44	4,74	0,59	1,70	0,54	2,90	5,33	0,06	0,15	30,00	8,00	7,00	6,00	6,00	6,00	90,00	25,00	239,00	120,00	760,00	398,00	63,00	24,00	28,00	5,02		91,00	187,00	0,50	Norddalen
K072.85S	70,69	14,98	0,29	1,93	1,48	0,64	4,53	4,80	0,04	0,07	32,00	3,00	3,00	6,00	8,00	5,00	21,00	14,00	138,00	372,00	983,00	174,00	15,00	15,00	19,00	3,41	2,00	33,00	65,00	0,50	Norddalen
K143.85	71,94	15,27	1,31	0,17	1,74	0,42	6,59	1,52	0,04	0,05	15,00	4,00	3,00	2,00	1,00	4,00	17,00	11,00	34,00	490,00	719,00	112,00	11,00	9,00	12,00	2,00	3,00	43,50	84,40	1,00	Gautelisvann
K145.85	72,55	14,53	1,35	0,18	0,76	0,32	4,13	5,64	0,03	0,05	19,00	4,00	1,00	2,00	2,00	2,00	34,00	14,00	106,00	229,00	1101,00	107,00	10,00	8,00	7,00	1,26	1,00	18,00	25,00	0,50	Gautelisvann
ES022GR	72,97	13,85	2,48	0,26	1,21	0,23	3,10	5,76	0,04	0,03	10,00	1,00	7,00	8,00	7,00	1,00	70,00	27,00	246,00	103,00	599,00	309,00	57,00	19,00	30,00	5,38	0,50	97,00	204,00	0,50	Norddalen
ES033GR	75,32	13,70	1,48	0,20	0,97	0,19	3,20	5,56	0,03	0,02	10,00	1,00	6,00	2,00	1,00	1,00	14,00	22,00	230,00	118,00	500,00	199,00	26,00	16,00	52,00	11,00	5,00	73,90	154,00	1,00	Norddalen
K272.3N	76,65	12,48	1,35	0,09	0,74	0,07	3,30	5,29	0,01	0,01	5,00	1,00	6,00	2,00	1,00	9,00	38,00	63,00	391,00	24,00	80,00	168,00	142,00	17,00	52,00	9,33	0,50	106,00	170,00	2,00	Norddalen
ES024GR	76,91	12,44	1,70	0,14	0,78	0,15	3,10	5,43	0,02	0,01	5,00	1,00	1,00	2,00	1,00	1,00	45,00	30,00	319,00	46,00	214,00	214,00	76,00	15,00	43,00	7,71	0,50	80,00	168,00	0,50	Norddalen